

1 **Ocean acidification impacts bacteria-phytoplankton**
2 **coupling at low nutrient-conditions**

3

4 **Thomas Hornick¹, Lennart T. Bach², Katharine J. Crawford³, Kristian Spilling^{4,5},**
5 **Eric P. Achterberg^{2,6}, Jason N. Woodhouse¹, Kai G. Schulz^{2,7}, Corina P. D.**
6 **Brussaard^{3,8}, Ulf Riebesell², Hans-Peter Grossart^{1,9}**

7

8 [1]{Leibniz Institute of Freshwater Ecology and Inland Fisheries (IGB), Experimental
9 Limnology, 16775 Stechlin, Germany}

10 [2]{GEOMAR Helmholtz Centre for Ocean Research Kiel, Düsternbrooker Weg 20, 24105
11 Kiel, Germany}

12 [3]{ NIOZ Royal Netherlands Institute for Sea Research, Department of Marine Microbiology
13 and Biogeochemistry, and Utrecht University, P.O. Box 59, 1790 AB Den Burg, Texel, The
14 Netherlands}

15 [4]{Marine Research Centre, Finnish Environment Institute, P.O. Box 140, 00251 Helsinki,
16 Finland}

17 [5]{Tvärminne Zoological Station, University of Helsinki, J. A. Palménin tie 260, 10900
18 Hanko, Finland}

19 [6]{National Oceanography Centre Southampton, European Way, University of Southampton,
20 Southampton, SO14 3ZH, UK}

21 [7]{Southern Cross University, P.O. Box 157, Lismore, NSW 2480, Australia}

22 [8]{Aquatic Microbiology, Institute for Biodiversity and Ecosystem Dynamics, University of
23 Amsterdam, P.O. Box 94248, 1090 GE Amsterdam, The Netherlands}

24 [9]{Potsdam University, Institute for Biochemistry and Biology, 14469 Potsdam,
25 Maulbeerallee 2, Germany}

26 Correspondence to: T. Hornick (hornick@igb-berlin.de)

27

28 **Abstract**

29 The oceans absorb about a quarter of the yearly produced anthropogenic atmospheric carbon
30 dioxide (CO₂), resulting in a decrease in surface water pH, a process termed ocean
31 acidification (OA). Surprisingly little is known about how OA affects the physiology of
32 heterotrophic bacteria or the coupling of heterotrophic bacteria to phytoplankton when
33 nutrients are limited. Previous experiments were, for the most part, undertaken during
34 productive phases or following nutrient additions designed to stimulate algal blooms.
35 Therefore, we undertook an *in situ* large-volume mesocosm (~55 m³) experiment in the Baltic
36 Sea by simulating different fugacities of CO₂ (*f*CO₂) extending from present to future
37 conditions. The study was conducted in July-August after the nominal spring-bloom, in order
38 to maintain low-nutrient conditions throughout the experiment. This resulted in phytoplankton
39 communities dominated by small-sized functional groups (picophytoplankton). There was no
40 consistent *f*CO₂-induced effect on Bacterial Protein Production (BPP), cell-specific BPP
41 (csBPP) or biovolumes (BVs) of either FL or PA heterotrophic bacteria, when considered as
42 individual components (univariate analyses). Permutational Multivariate Analysis of Variance
43 (PERMANOVA) revealed a significant effect of the *f*CO₂-treatment on entire assemblages of
44 dissolved and particulate nutrients, metabolic parameters and the bacteria-phytoplankton
45 community. However, distance-based linear modelling only identified *f*CO₂ as a factor
46 explaining the variability observed amongst the microbial community composition, but not
47 for explaining variability within the metabolic parameters. This suggests that *f*CO₂ impacts on
48 microbial metabolic parameters occurred indirectly through varying physiochemical
49 parameters and microbial species composition. Cluster analyses examining the co-occurrence
50 of different functional groups of bacteria and phytoplankton further revealed a separation of
51 the four *f*CO₂-treated mesocosms from both control mesocosms, indicating that complex
52 trophic interactions might be altered in a future acidified ocean. Possible consequences for
53 nutrient cycling and carbon export are still largely unknown, in particular in a nutrient limited
54 ocean.

55

56 **Key words**

57 Ocean acidification, CO₂ enrichment, trophic interaction, Baltic Sea, KOSMOS mesocosm
58 experiment, bacterial production, phytoplankton

59 1 Introduction

60 Since the industrial revolution the oceans have absorbed ca. one half of the anthropogenic
61 carbon dioxide (CO₂). This has resulted in a shift in carbonate equilibria and pH (Caldeira and
62 Wickett, 2003; Raven et al., 2005; Sabine et al., 2004), with potential consequences for
63 organismal physiology (Fabry et al., 2008, Taylor et al., 2012). In principal, autotrophs should
64 be fertilized by an enhanced CO₂ availability, increasing the production of particulate (POM)
65 and dissolved organic matter (DOM) (Hein and Sand-Jensen, 1997; Egge, et al., 2009; Losh et
66 al., 2012; Riebesell et al., 2007). However, most CO₂ enrichment experiments studying
67 natural plankton assemblages under variable nutrient conditions do not reveal a consistent
68 response of primary production to elevated CO₂ (e.g. Engel, et al., 2005; Riebesell et al.,
69 2007; Hopkinson et al., 2010). Both the amount and the stoichiometric composition of algal
70 DOM and POM can be affected by changes in *f*CO₂. For example, Riebesell et al. (2007) and
71 Maat et al. (2014) reported an increased stoichiometric drawdown of carbon (C) to nitrogen
72 (N) at higher levels of *f*CO₂, most likely as a result from C-overconsumption (Toggweiler,
73 1993).

74 Heterotrophic bacteria, in oligotrophic systems, are largely dependent on phytoplankton
75 derived organic carbon (e.g. Azam, 1998), and as such respond to alterations in both the
76 quantity and quality of phytoplankton derived DOM and POM (e.g. Allgaier et al., 2008;
77 Grossart et al., 2006a, de Kljijver et al., 2010). Availability and competition for nutrients,
78 however, can substantially impact *f*CO₂-induced changes in activity and biomass of
79 phytoplankton and subsequently of heterotrophic bacteria. In nutrient-depleted or nutrient-
80 limited systems, bacteria are restricted in their utilization of phytoplankton derived organic
81 carbon (Hoikkala et al., 2009; Lignell et al., 2008; Thingstad and Lignell, 1997).
82 Consequently, *f*CO₂ dependent increases in inorganic C-availability for autotrophs may not
83 stimulate heterotrophic activity, causing a decoupling of heterotrophic and autotrophic
84 processes (Thingstad et al., 2008). The accumulation of bioavailable dissolved organic carbon
85 (DOC) and particulate organic carbon (POC), as a consequence of this decoupling in nutrient
86 limited oceanic surface waters, may have profound consequences for nutrient cycling and the
87 nature of the oceanic carbon pump (Cauwet et al., 2002; Mauriac et al., 2011; Søndergaard et
88 al., 2000; Thingstad et al., 1997). Given that various studies have reported on limitation of
89 bacterial growth by inorganic nutrients in several parts of the Baltic Sea (e.g. Hoikkala et al.,
90 2009; Kivi et al., 1993; Kuparinen and Heinänen, 1993; Zweifel et al. 1993), we sought to

91 evaluate the effects of enhanced $f\text{CO}_2$ on activity and biomass of free-living (FL) as well as
92 particle associated (PA) bacteria during a period characterised by low nutrients and low
93 productivity.

94

95 **2 Methods**

96 **2.1 Experimental setup, CO_2 manipulation and sampling**

97 Nine floating, pelagic KOSMOS (Kiel Off-Shore Mesocosms for future Ocean Simulations;
98 Riebesell et al., 2013a, Riebesell, et al., 2013b) mesocosms (cylindrical, 2 m diameter, 17 m
99 long with conical sediment trap extending to 19 m depth) were moored on 12th June 2012 (day
100 -10 = t-10; 10 days before CO_2 manipulation) at 59°51.5'N, 23°15.5'E in the Baltic Sea at
101 Tvärminne Storfjärden on the south-west coast of Finland. Exposed mesocosm bags were
102 rinsed for a period of five days, covered on the top and bottom with a 3 mm net to exclude
103 larger organisms. Thereby, the containing water was fully exchanged with the surrounding
104 water masses. Five days prior the start of the experiment (t-5), sediment traps were attached to
105 the bottom of each mesocosm at 17 m depth. In addition, submerged mesocosm bags were
106 drawn 1.5 m above the water surface, enclosing and separating ~55 m³ of water from the
107 surrounding Baltic Sea and meshes were removed. Mesocosms were covered by a
108 photosynthetic active radiation (PAR) transparent roof to prevent nutrient addition from birds
109 and freshwater input from rain. Additionally, existing haloclines were removed in each
110 mesocosm as described in Paul et al. (2015), thereby creating a fully homogeneous water
111 body.

112 The experiment was conducted between 17th June (t-5) and 4th August (t43) 2012. To
113 minimize environmental stress on enclosed organisms CO_2 addition was performed stepwise
114 over three days commencing on day t0. CO_2 addition was repeated at t15 in the upper mixed
115 7 m to compensate for outgassing. Different $f\text{CO}_2$ treatments were achieved by equally
116 distributing filtered (50 μm), CO_2 -saturated seawater into the treated mesocosms with a water
117 distributor as described by Paul et al. (2015). Control mesocosms were also manipulated with
118 the water distributor and 50 μM pre-filtered water without CO_2 . CO_2 amendments resulted in
119 ca. 0.04-0.35 % increases in the total water volume across mesocosms (Paul et al. 2015).
120 Integrated water samples (0-17 m) were collected from each mesocosm and the surrounding

121 seawater using depth-integrated water samplers (IWS, HYDRO-BIOS, Kiel). Samples for
122 activity measurements were directly subsampled from the IWS on the sampling boat without
123 headspace to maintain in-situ $f\text{CO}_2$ concentrations during incubation.

124 Unfortunately, three mesocosms failed during the experiment, as a consequence of welding
125 faults, resulting in unquantifiable water exchanges with the surrounding waters. Therefore,
126 with reference to the six remaining mesocosms, CO_2 concentrations defining each treatment
127 are reported as the mean $f\text{CO}_2$ concentration determined over the initial 43 days (t1-t43) as
128 described in Paul et al. (2015). The control mesocosms (two replicates) had 365 μatm and 368
129 μatm $f\text{CO}_2$, respectively. The four treatment mesocosms each had 497 μatm , 821 μatm , 1007
130 μatm and 1231 μatm $f\text{CO}_2$, respectively. Detailed descriptions on the study site, mesocosm
131 deployment and system, performance of the mesocosm facility throughout the experiment,
132 CO_2 addition, carbonate chemistry, cleaning of the mesocosm bags as well as sampling
133 frequencies of single parameters are given in Paul et al. (2015).

134 **2.2 Physical and chemical parameters**

135 Physical measurements (i.e. temperature and salinity) were performed using a CTC60M
136 memory probe (Sea and Sun Technology, Trappenkamp, Germany) and are calculated as the
137 mean, integrated over the total depth. Photosynthetic active radiation (PAR) was measured
138 with a PAR sensor (LI-COR LI-192) at the roof of Tvärminne Zoological Station.

139 Samples for dissolved inorganic carbon concentrations (DIC) and total pH were gently
140 pressure-filtered (Sarstedt Filtropur PES, 0.2 μm pore size) using a membrane pump
141 (Stepdos). Total pH was determined as described in Dickson et al. (2007) on a Cary 100
142 (Varian) spectrophotometer in a temperature-controlled 10 cm cuvette using a *m*-cresol
143 indicator dye (Mosley et al., 2004). DIC concentrations were determined by infrared
144 absorption using a LI-COR LI-7000 on an AIRICA system (MARIANDA, Kiel). Total pH
145 and DIC were used to calculate carbonate chemistry speciation using the stoichiometric
146 equilibrium constants for carbonic acid of Mehrbach et al. (1973) as refitted by Lueker et al.
147 (2000).

148 Samples for dissolved organic carbon (DOC), total dissolved nitrogen (TDN) as well as
149 dissolved silica (DSi) and dissolved inorganic phosphate (DIP) were filtered through pre-
150 combusted (450 °C, 6h) GF/F filters (Whatman, nominal pore size of 0.7 μm). Concentrations

151 of DOC and TDN were determined using a high-temperature catalytic combustion technique
152 with a Shimadzu TOC-TN V analyser following Badr et al. (2003). DSi concentrations were
153 determined using standard colorimetric techniques (Grasshoff et al. 1983) at the micromolar
154 level with a nutrient autoanalyser (Seal Analytical, Quattro). DIP concentrations were
155 determined with a colorimetric method using a 2 m liquid waveguide capillary cell (Patey et
156 al., 2008, Zhang and Chi, 2002) with a miniaturised detector (Ocean Optics Ltd).

157 Total particulate carbon (TPC), particulate organic nitrogen (PON) and total particulate
158 phosphorus (TPP) samples were collected onto pre-combusted (450 °C, 6h) GF/F filters
159 (Whatman, nominal pore size of 0.7 µm) using gentle vacuum filtration and stored in glass
160 Petri dishes at -20 °C. Biogenic silica (BSi) samples were collected on cellulose acetate filters
161 (0.65 µm, Whatman) using gentle vacuum filtration (< 200 mbar) and stored in glass Petri
162 dishes at -20 °C. Filters for TPC/PON analyses were dried at 60 °C, packed into tin capsules
163 and measured on an elemental analyser (EuroEA) according to Sharp (1974), coupled by
164 either a Conflo II to a Finnigan Delta^{Plus} isotope ratio mass spectrometer or a Conflo III to a
165 Thermo Finnigan Delta^{Plus} XP isotope ratio mass spectrometer. Filters for TPP were treated
166 with oxidizing decomposition reagent (MERCK, catalogue no. 112936) to oxidise organic
167 phosphorus to orthophosphate. Particulate silica was leached from filtered material.
168 Concentrations of dissolved inorganic phosphate as well as dissolved silica were determined
169 spectrophotometrically according to Hansen and Koroleff (1999).

170 Samples for chlorophyll *a* (Chl *a*) were filtered on GF/F filters (Whatman, nominal pore size
171 of 0.7 µm) and stored at -20 °C. Chl *a* was extracted in acetone (90 %) and samples
172 homogenized. After centrifugation (10 min, 800 x g, 4 °C) the supernatand was analysed on a
173 fluorometer (TURNER 10-AU) to determine concentrations of Chl *a* (Welschmeyer, 1994).

174 Further details on the determination of physical parameters, concentration of Chl *a* as well as
175 dissolved and particulate nutrients can be obtained from Paul et al. (2015).

176 **2.3 Microbial standing stock**

177 Abundance of free-living (FL) heterotrophic prokaryotes (HP) and photoautotrophic
178 prokaryotic (*Synechococcus* spp.) as well as eukaryotic cells (<20 µm) were determined by
179 flow cytometry (Crawford et al. 2016). Briefly, phytoplankton were discriminated based on
180 their chlorophyll red autofluorescence and/or phycoerythrin orange autofluorescence (Marie

181 et al., 1999). In combination with their side scatter signal and size fractionation the
182 phytoplankton community could be divided into 6 clusters, varying in size from 1 to 8.8 μm
183 average cell diameter (Crawford et al., 2016). Three groups of picoeukaryotic phytoplankton
184 (Pico I-III), 1 picoprokaryotic photoautotroph (*Synechococcus* spp.) and 2 nanoeukaryotic
185 phytoplankton groups were detected. Biovolume (BV) estimations were based on cell
186 abundance and average cell diameters by assuming a spherical cell shape. The BV sum of
187 *Synechococcus* and Pico I-III is expressed as BV_{Pico} . The BV sum of Nano I and II will be
188 referred as BV_{Nano} .

189 Abundances of FL prokaryotes were determined from 0.5 % glutaraldehyde fixed samples
190 after staining with the nucleic acid-specific dye SYBR green I (Crawford et al. 2016).
191 Unicellular cyanobacteria (*Synechococcus* spp.) contributed maximally 10% of the total
192 counts. Two additional groups were identified based on their low (LDNA) and high (HDNA)
193 fluorescence. This identification was based on gating of SYBR green I fluorescence against
194 the side scatter signal (Brussaard, 2004 with adaptation according to Mojica et al., 2014).
195 Particle-associated (PA) prokaryotes were enumerated by epifluorescence-microscopy on a
196 Leica Leitz DMRB fluorescence microscope with UV- and blue light excitation filters (Leica
197 Microsystems, Wetzlar, Germany). Fresh samples were gently mixed to prevent particle
198 settling and a 15 mL subsample was filtered on a 0.1-% Irgalan Black coloured 5.0 μm
199 polycarbonate-filter (Whatman, Maidstone, UK) (Hobbie et al., 1977). Filters were fixed with
200 glutaraldehyde (Carl Roth, Karlsruhe, Germany, final conc. 2 %) and stained for 15 min with
201 4'-diamidino-2-phenylindole (DAPI, final conc. 1 $\mu\text{g mL}^{-1}$) (Porter and Feig, 1980) directly
202 on the filtration device and rinsed twice with sterile filtered habitat water before air-drying
203 and embedding in Citifluor AF1 (Citifluor Ltd, London, UK) on a microscopic slide (Rieck et
204 al., 2015). Counts were made based on 15 random unique squares as observed at a
205 magnification of 1000x. The total number of heterotrophic PA prokaryotes was enumerated
206 by subtracting Chl *a* autofluorescent cells from DAPI-stained cells.

207 BV of FL and PA prokaryotes were calculated separately. For FL prokaryotes we estimated
208 BVs on the basis of an average cell volume of 0.06 μm^3 (Hagström et al., 1979). BV of PA
209 prokaryotes were calculated from measurements of 1600 cells across 3 different mesocosms
210 (346 μatm , 868 μatm , 1333 μatm) and three time points (t0, t20, t39) throughout the
211 experiment (Massana et al., 1997). A resulting average BV of 0.16 μm^3 per cell was used to
212 calculate BV of PA prokaryotes derived from cell abundances. We subsequently adopted the

213 term “heterotrophic bacteria”, since bacteria account for the majority of non- photosynthetic
214 prokaryotes in surface waters (Karner et al., 2001; Kirchman et al. 2007).

215 **2.4 Metabolic parameters**

216 Rates of bacterial protein production (BPP) were determined by incorporation of ^{14}C -leucine
217 (^{14}C -Leu, Simon and Azam, 1989) according to Grossart et al. (2006a). Triplicates and a
218 formalin-killed control were incubated with ^{14}C -Leu (213 mCi mmol^{-1} ; Hartmann Analytic
219 GmbH, Germany) at a final concentration of 165 nM, which ensured saturation of the uptake
220 systems of both FL and PA bacteria. Incubation was performed in the dark at *in situ*
221 temperature (between 7.8 °C and 15.8 °C) for 1.5 h. After fixation with 2% formalin, samples
222 were filtered onto 5.0 μm (PA bacteria) nitrocellulose filters (Sartorius, Germany) and
223 extracted with ice-cold 5% trichloroacetic acid (TCA) for 5 min. Thereafter, filters were
224 rinsed twice with ice-cold 5% TCA, once with ethanol (50% v/v), and dissolved in
225 ethylacetate for measurement by liquid scintillation counting (Wallac 1414, Perkin Elmer).
226 Afterwards, the collected filtrate was filtered on 0.2 μm (FL bacteria) nitrocellulose filters
227 (Sartorius, Germany) and processed in the same way as the 5.0 μm filters. Standard deviation
228 of triplicate measurements was usually <15%. The amount of incorporated ^{14}C -Leu was
229 converted into BPP by using an intracellular isotope dilution factor of 2. A conversion factor
230 of 0.86 was used to convert the produced protein into carbon (Simon and Azam, 1989). Cell-
231 specific BPP rates (csBPP) were calculated by dividing BPP-rates by abundances of FL
232 prokaryotes and PA HP.

233 Community respiration (CR) rates were calculated from oxygen consumption during an
234 incubation period of 48 hours at *in situ* temperature in the dark by assuming a respiratory
235 quotient of 1 (Berggren et al., 2012). Thereby oxygen concentrations were measured in
236 triplicate in 120 mL O_2 bottles without headspace, using a fiber optical dipping probe
237 (PreSens, Fibox 3), which was calibrated against anoxic and air saturated water.

238 Primary production (PP) was measured using radio-labeled $\text{NaH}^{14}\text{CO}_3$ (Steeman-Nielsen,
239 1952) from 0-10 m depth integrated samples. After incubation of duplicate samples with
240 10 μL of ^{14}C bicarbonate solution (DHI Lab, 20 $\mu\text{Ci mL}^{-1}$) in 8 mL vials at 2,4,6, 8 and 10 m
241 for 24 h, samples were acidified with 1 M HCl to remove remaining inorganic ^{14}C .
242 Radioactivity was determined by using a scintillation counter (Wallac 1414, Perkin Elmer).

243 PP was calculated knowing the dark-control corrected ^{14}C incorporation and the fraction of
244 the ^{14}C addition to the total inorganic carbon pool according to Gargas (1975). Further
245 descriptions on the measurement of CR and PP are given by Spilling et al. (2016a).

246 **2.5 Statistical analyses**

247 Permutational multivariate analysis of variance – PERMANOVA (Anderson, 2001, McArdle
248 and Anderson, 2001) was used to determine associations between physical/chemical variables
249 and biotic variables. PERMANOVA (perm=9999) was performed to test for significant
250 differences in variance over time and between $f\text{CO}_2$ -treated mesocosms (Anderson et al.,
251 2008). Environmental data were normalized according Clarke and Gorley (2001). Biotic
252 abundance data were $\log(x+1)$ transformed (Clarke and Green, 1988). PERMANOVA
253 partitions the total sum of squares based on the experimental design and calculates a distance
254 based pseudo- F statistic for each term in the model. Distance-based linear modeling (DistLM)
255 was implemented to relate physical/chemical predictor variables and the multivariate
256 assemblage of biotic variables (Supplementary Table S1) (Legendre and Anderson, 1999;
257 McArdle and Anderson, 2001; Anderson et al., 2008). The DistLM routine was based on the
258 AIC model selection criterion (Akaike, 1973, Akaike, 1974, Burnham and Anderson, 2004)
259 using a step-wise selection procedure. In case of equally AIC-ranked models (difference <1),
260 a model with fewer parameters was preferred. Unconstrained ordination methods were used to
261 visualize and determine effects of $f\text{CO}_2$ on biotic and physical/chemical variables in
262 multivariate space, thereby maximizing the total overall variation (Anderson et al., 2008). A
263 Principal Component Analysis (PCA) was performed on normalized chemical data to identify
264 chemical gradients and patterns between the differently $f\text{CO}_2$ -treated mesocosms over time
265 (Mardia et al., 1979; Venerables and Ripley, 2002). Distance based redundancy analysis
266 (dbRDA) was used for visual interpretation of the DistLM in multi-dimensional space
267 (Anderson et al., 2008). Multivariate analyses of physicochemical, metabolic and community
268 data were performed on a reduced data set comprising 10 time points (t5-t29, every 3rd day,
269 t31), containing all measured activity variables (BPP, areal PP and CR). Missing values of
270 nutrient data or abundance data (based on every other day measurements) were estimated as
271 means of the preceding and following measurement day. No activity data were interpolated or
272 data extrapolated in general.

273 Cluster analyses were performed based on Spearman's rank correlation coefficients calculated
274 for each mesocosm between all possible combinations of LDNA, HDNA, pico- and
275 nanophytoplankton abundances as well as total Chl *a*. Thereafter, *p*-values were corrected for
276 multiple testing according Benjamini and Hochberg (1995). The R-package pvclust was used
277 to assess the uncertainty in hierarchical cluster analysis (Suzuki and Shimodeira, 2015). For
278 each cluster, AU (approximately unbiased) *p*-values (between 0 and 1) were calculated via
279 multiscale bootstrap resampling (Suzuki and Shimodaira, 2015).

280 PERMANOVA, distLM and dbRDA were carried out using Primer 6.0 and PERMANOVA +
281 for PRIMER software (Clarke and Gorley, 2006, Anderson et al., 2008). All other analysis,
282 including PCA and the visualisation of result was performed with R 3.2.5 (R Core Team,
283 2016) using packages Hmisc (Harrell et al., 2016), vegan (Oksanen et al., 2016), pvclust
284 (Suzuki and Shimodeira, 2015), gplots (Warnes et al., 2016) and ggplot2 (Wickham, 2009).

285

286 **3 Results**

287 **3.1 Bacterial production (BPP) and biovolume (BV)**

288 Heterotrophic bacterial BV was comprised predominantly of FL bacteria. PA bacteria
289 contributed maximally $2 \pm 0.7 - 10 \pm 0.7 \%$ (mean $4.8 \pm 0.6 \%$) of total bacterial BV. PA
290 bacteria, however, accounted for a substantial fraction of overall BPP ($27 \pm 1 - 59 \pm 7 \%$,
291 mean $39 \pm 4 \%$). There was no significant effect of $f\text{CO}_2$ on BPP, csBPP or BV of neither
292 FL nor PA heterotrophic bacteria ($p_{\text{perm}} > 0.05$), however a significant temporal effect was
293 observed ($p_{\text{perm}} < 0.05$). Both bacterial size-fractions had distinct dynamics in abundance,
294 BPP and csBPP during the course of the experiment. BPP and bacterial abundances were
295 closely related to Chl *a* and BV of nano- and picophytoplankton, trending along with Chl *a*
296 until t10 and then continuing to increase with BVs of nanophotoautotrophs and Chl *a*. The
297 period between t16 and t26, following a sharp decrease in Chl *a* at t16 revealed highest BPP
298 rates across the experiment with lower rates at higher $f\text{CO}_2$ for PA as well as FL bacteria.
299 CsBPP-rates were lower at elevated $f\text{CO}_2$ for only the FL bacteria during this period.
300 Additionally, BVs of FL and PA bacterial revealed contrasting dynamics (Fig. 1, Fig. S1).
301 PA bacterial BVs declined with the decay of Chl *a*, whereas FL BVs increased strongly
302 associated with an increase in BV of picophotoautotrophs during this period. The ratio of

303 HDNA:LDNA prokaryotes, which both making up FL bacteria, showed also differences
304 between the experimental treatments. Between t14-t25 the ratio of HDNA:LDNA was lower
305 at higher $f\text{CO}_2$.

306 **3.2 Phytoplankton dynamics**

307 Chl *a* concentration exhibited distinct maxima at two time periods (t5 and t16). The second
308 maximum was associated with an increase in the BV of nanophotoautotrophs (BV_{Nano}) (Fig.
309 2). This increase was reduced in mesocosms containing higher concentrations of $f\text{CO}_2$
310 between t13-t17. The differences in BV_{Nano} between the treatments were reflected in lower
311 concentrations of Chl *a* in the 3 highest $f\text{CO}_2$ -treated mesocosms at t16. Chl *a* and BV_{Nano}
312 concentrations declined after t16. In contrast, BV of picophotoautotrophs (BV_{Pico}) increased
313 after t11, associated with an increase in BV of *Synechococcus* spp., which accounted for
314 $31 \pm 2 \%$ to $59 \pm 2 \%$ of BV_{Pico} across the period of this study (Fig. S2). All four groups of
315 picoautotrophs distinguished by flow cytometry, exhibited time-dependent positive or
316 negative relationships with $f\text{CO}_2$ (Fig. 3, Fig. S2, Fig. S3). The Pico I ($\sim 1 \mu\text{m}$) and Pico II
317 taxa infrequently exhibited strong fertilization effects in response to the $f\text{CO}_2$ -treatment. In
318 contrast, *Synechococcus* spp. and Pico III were infrequently negatively affected by the $f\text{CO}_2$ -
319 treatment.

320 **3.3 Relation between functional heterotrophic and autotrophic groups**

321 A cluster analysis of pairwise Spearman correlations between functional bacterial and
322 phytoplankton groups revealed a separation based on $f\text{CO}_2$ -treatment. Specifically the four
323 CO_2 amended mesocosms were readily distinguishable from the control treatments. Multiple
324 bootstrap resampling (Suzuki and Shimodaira, 2015) supported this, but only significantly for
325 the two highest $f\text{CO}_2$ -treated mesocosms. The two highest $f\text{CO}_2$ -treatments revealed a positive
326 correlation of LDNA bacteria and Pico I, which could not be observed in any other
327 experimental treatment. In all CO_2 -treated mesocosm we observed positive correlations
328 between *Synechococcus* spp. and Pico III as well as *Synechococcus* spp. and Pico I, which
329 were not present in both control mesocosms. In contrast positive correlations between LDNA
330 and HDNA were not detected in any $f\text{CO}_2$ -treatment. Additionally positive correlations
331 between Pico and Nano II as well as HDNA and Cyanobacteria were only present in both
332 controls and the lowest $f\text{CO}_2$ -treatment (Fig. 4).

333 After t10, the ratio between heterotrophic prokaryotic BV and Chl *a* varied between the $f\text{CO}_2$ -
334 treatments, but did not show a consistent pattern. After t17, however, the control mesocosms
335 revealed a higher ratio compared to all $f\text{CO}_2$ -treated mesocosms (Fig. 5).

336 **3.4 Multivariate physicochemical characterisation**

337 Integrated water temperature and PAR ranged between 8.0 - 15.9 °C and 11.2 - 66.8 mol m⁻²
338 day⁻¹ during the experiment, respectively. Integrated water temperature reached the maximum
339 at t15 and dropped again to 8.2 °C at t31.

340 PERMANOVA results (Table 1) on a multivariate assemblage of dissolved (DOC, TDN,
341 Phosphate, Bsi) and particulate (TPC, PON, POP, PBsi) nutrients showed significant temporal
342 (Time- $F_{9,10}=11.1$, $p=0.0001$) and spatial variations along the $f\text{CO}_2$ -gradient ($f\text{CO}_2$ - $F_{4,10}=2.6$,
343 $p=0.02$). PCA ordination of the same chemical dataset strongly reflects the temporal pattern,
344 separating the initial time points before t11 from other time points of the experiments along
345 the first PCA axis (Fig. 6). Thereby, Eigenvectors of TPC and PON loaded highest on PCA
346 axis 1 (Table 2). PCA axis two was mainly characterized by high eigenvectors of dissolved
347 phosphate as well as dissolved and particulate silica. The first two PCA axes explained 69 %
348 of variation and cumulatively 80% with including axis three (Table 2).

349 **3.5 Multivariate characterisation of metabolic parameters**

350 PERMANOVA on the resemblance matrix of normalized metabolic variables (BPP, areal PP,
351 CR) revealed significant temporal (Time- $F_{9,10}=6.7$, $p=0.0002$) and spatial variations along the
352 $f\text{CO}_2$ -gradient ($f\text{CO}_2$ - $F_{4,10}=2.64$, $p<0.03$) (Table 3). DistLM identified significant effects of
353 Temperature ($p<0.03$), Phosphate ($p<0.02$), DOC ($p<0.05$) and Pbsi ($p<0.02$) on the
354 multivariate assemblage of metabolic variables (Table 4). The step-wise procedure selects
355 PAR, temperature, DOC and phosphate as determining factors (AIC=59.6; $R^2=0.26$; number
356 of variables=4). The dbRDA ordination separates the temporal development. Thereby, 92 %
357 of the variability in the fitted model and 24 % of the total variation is explained by the first
358 two dbRDA axes (Fig. 6).

359 **3.6 Multivariate characterisation of the bacterioplankton and phytoplankton** 360 **community**

361 PERMANOVA on the resemblance matrix of a multivariate assemblage comprising variables
362 of bacterial and phytoplankton communities (abundances of Pico I-III, Nano I-II, FL bacteria
363 (HDNA, LDNA), PA bacteria, Cyanobacteria and Chl *a*) revealed significant temporal (Time-
364 $F_{9,10}=56.8$, $p=0.0001$) and spatial variations along the $f\text{CO}_2$ -gradient ($f\text{CO}_2$ - $F_{4,10}=14.9$,
365 $p=0.0001$) (Table 5). DistLM identified significant effects of $f\text{CO}_2$ ($p<0.02$), Temperature
366 ($p<0.001$), Phosphate ($p<0.003$), TPC ($p<0.001$), Pbsi ($p<0.001$) and POP ($p<0.001$) on the
367 multivariate assemblage of bacterial and phytoplankton community (Table 6). The step-wise
368 procedure selects $f\text{CO}_2$, temperature, TPC and phosphate as determining factors (AIC=67.2;
369 $R^2=0.44$; number of variables=4). The dbRDA reveals a separation along the gradient of $f\text{CO}_2$
370 on the second dbRDA axis. The first dbRDA axis represents the overall temporal
371 development. Thereby the first two dbRDA axis capture 74 % of the variability in the fitted
372 model and 32 % of the total variation.

373

374 **4 Discussion**

375 Although OA and its ecological consequences have received growing recognition during the
376 last decade (Riebesell and Gattuso, 2015), surprisingly little is known about the ecological
377 effects on heterotrophic bacterial biomass, production or the coupling of bacterio- and

378 phytoplankton at nutrient limited conditions. Previous experiments were, for the most part,
379 conducted during productive phases of the year (e.g. phytoplankton blooms), under eutrophic
380 conditions (e.g. coastal areas) or with nutrient additions (Grossart et al., 2006a; Allgaier et al.,
381 2008; Brussaard et al., 2013; Lindh et al., 2013; Bach et al, 2016). However, large parts of the
382 oceans are nutrient-limited or experience extended nutrient-limited periods during the year
383 (Moore et al., 2013). Thus, we conducted our experiment in July-August, when nutrients and
384 phytoplankton production were relatively low in the northeastern Baltic Sea (Hoikkala et al.,
385 2009; Lignell et al., 2008) and exposed a natural plankton community to different levels of
386 CO₂.

387 **4.1 Phytoplankton-bacterioplankton coupling at low nutrient conditions**

388 Heterotrophic bacteria are important recyclers of autochthonous DOM in aquatic systems and
389 play an important role in nutrient remineralisation in natural plankton assemblages (Kirchman
390 1994, Brett et al., 1999). BV and production of heterotrophic bacteria are highly dependent on
391 quantity and quality of phytoplankton-derived organic carbon and usually are tightly related
392 to phytoplankton development (Grossart et al., 2003; Grossart et al., 2006b; Rösler and
393 Grossart, 2012; Attermeyer et al., 2014; Attermeyer et al., 2015). During this study, low
394 nitrogen availability limited overall autotrophic production (Paul et al., 2015, Nausch et al.,
395 2016). This resulted in a post spring bloom phytoplankton community, dominated by
396 picophytoplankton (Paul et al., 2015). This is consistent with previous reports of
397 picophytoplankton accounting for a large fraction of total phytoplankton biomass in
398 oligotrophic, nutrient poor systems (e.g. Platt et al., 1983; Agawin et al., 2000). Chl *a*
399 dynamics indicated two minor blooms of larger phytoplankton during the first half of the
400 experiment, although picophytoplankton still accounted for mostly >50 % of the total Chl *a*
401 during this period (Paul et al., 2015, Spilling et al., 2016b). The phytoplankton development
402 was also reflected in the PCA ordination of dissolved and particulate nutrients, clearly
403 separating the preceding period before t11, including the first peak of Chl *a*, from the other
404 observations during the experiment on principal component 1 (Fig. 6). The separation was
405 primarily driven by concentrations of particulate matter (Table 2), which decreased until t11
406 and subsequently sank out of the water column (Paul et al., 2015).

407 Bacterial BV and BPP paralleled phytoplankton development during this period. With the
408 decay of the initial phytoplankton bloom, a second bloom event comprised primarily of

409 nanophytoplankton and picophytoplankton resulted (Crawford et al., 2016). A decrease in
410 nanophytoplankton BV and Chl *a* concentrations after t16/t17, benefitted both FL
411 heterotrophic bacteria and picophotoautotrophs. The increased availability of DOM, resulting
412 from cell lysis and remineralisation of POM was associated with increases in the BV of both
413 groups and bacterial production levels (Fig. 1, Fi. S1). We attributed these increases to the
414 cells of Picoplankton which, due to their high volume to surface ratio as well as a small
415 boundary layer surrounding these cells, are generally favoured compared to larger cells in
416 terms of resource acquisition at low nutrient conditions (Raven, 1998; Moore et al., 2013). If
417 cell size is the major factor determining the access to dissolved nitrogen and phosphorous,
418 bacteria should be able to compete equally or better with picophytoplankton at low
419 concentrations (Suttle et al., 1990; Drakare et al., 2003). However, when phytoplankton is
420 restricted in growth due to the lack of mineral nutrients, a strong comensalistic relationship
421 between phytoplanktonic DOM production and bacterioplanktonic DOM utilization may
422 evolve (Azam et al., 1983; Bratbak and Thingstad, 1985, Joint et al., 2002). Although
423 heterotrophic microbes may indirectly limit primary production by depriving phytoplankton
424 of nutrients, they would not be able to outcompete autotrophs completely since this would
425 remove their source of carbon and energy substrate (Bratbak and Thingstad, 1985, Joint et al.,
426 2002). Such a relationship might explain the paralleled increase in FL bacterial and
427 picophytoplankton BV.

428 PA bacteria are typically impacted to a lesser extent by nutrient limitation due to consistently
429 higher nutrient availability at particle surfaces (e.g. Grossart and Simon, 1993). This was
430 reflected in this study by the maintenance of high csBPP rates associated with PA
431 heterotrophic bacteria throughout the experiment. Overall, PA bacteria contributed only a
432 minor fraction (maximal $10 \pm 0.7\%$) to the overall bacterial BV, which is typical for
433 oligotrophic or mesotrophic ecosystems (Lapoussière et al., 2010). Nevertheless, the
434 substantial contribution of PA heterotrophic bacteria to overall BPP emphasizes their
435 importance, especially during such low productive periods (e.g. Simon et al., 2002; Grossart,
436 2010). PA heterotrophic bacteria are essential for the remineralization of nutrients from
437 autotrophic biomass, which would otherwise sink out from surface waters (Cho and Azam,
438 1988; Turley and Mackie, 1994). Leakage of hydrolysis products and the attachment and
439 detachment of bacteria to and from particles stimulate production amongst free-living bacteria
440 (Cho and Azam, 1988; Smith et al., 1992; Grossart et al., 2003) and picophytoplankton.

441 **4.2 Effects of $f\text{CO}_2$ /pH on phytoplankton-bacterioplankton coupling at low** 442 **nutrient conditions**

443 The response of heterotrophic bacteria to changes in $f\text{CO}_2$ have been previously shown to be
444 related to phytoplankton rather than being a direct effect of pH or CO_2 (e.g. Allgaier et al.,
445 2008, Grossart et al., 2006a). Here, neither BPP nor BV of neither FL nor PA bacteria
446 suggested a direct effect of CO_2 (PERMANOVA). Differences in FL bacterial BV, BPP, and
447 the ratio of HDNA/LDNA, occurred along the gradient of $f\text{CO}_2$, but were limited to short time
448 periods. Furthermore, these changes were not consistent with $f\text{CO}_2$ resulting in both increases
449 and decreases of a particular variable at specific times (Fig. 1). Periods where effects were
450 apparent comprised periods with high organic matter turnover (e.g. breakdown of Chl *a*
451 maximum). However, Paul et al. (2015) could not reveal any effect of $f\text{CO}_2$ on the export of
452 carbon, neither across the study period nor at individual time points. Thus it is reasonable to
453 speculate that these small $f\text{CO}_2$ -related differences in bacterial variables were a consequence
454 of other altered components of the aquatic food web, and thereby did not manifest as changes
455 in carbon export.

456 Given the inability to relate individual aspects of microbial metabolism or community
457 composition to $f\text{CO}_2$ concentrations, we sought to determine whether an impact was evident
458 using a multivariate approach. Chemical, metabolic and community matrices were shown to
459 exhibit large variations in relation to a strong temporal effect throughout the whole sampling
460 period ($p \ll 0.01$, Table 1, Table 3, Table 5). In addition, an effect of the $f\text{CO}_2$ -treatment was
461 also evident in all three multivariate assemblages, albeit explaining far less of the observed
462 variability in chemical and metabolic variables ($p < 0.03$, Table 1, Table 3, Table 5). However,
463 when relating physiochemical to metabolic variables (DistLM, Table 4), neither $f\text{CO}_2$ nor pH
464 were suitable to explaining the observed variability. In contrast, $f\text{CO}_2$ contributed to
465 explaining the variability amongst the bacterioplankton-phytoplankton community (DistLM,
466 Table 6). Taken together, this suggests that effects of $f\text{CO}_2$ -treatments manifest indirectly,
467 through either altering physiochemical parameters or more likely the composition of the
468 microbial community, as an impact on microbial metabolism.

469 **4.3 $f\text{CO}_2/\text{pH}$ effects on phytoplankton alter indirectly phytoplankton-**
470 **bacterioplankton coupling at low nutrient conditions**

471 Autotrophic organisms can be fertilized by an enhanced CO_2 availability, altering growth
472 conditions of phytoplankton and increasing the production of particulate (POM) and dissolved
473 organic matter (DOM) (Hein and Sand-Jensen, 1997; Egge, et al., 2009; Riebesell et al., 2007;
474 Losh et al., 2012). As a consequence of this increased photosynthetic fixation rate, both
475 quantity and quality of dissolved organic matter (DOM) available for heterotrophic bacteria
476 are impacted, with potential implications for the nature of coupling between phytoplankton
477 and bacterioplankton at low nutrient conditions (Azam et al., 1983; Bratbak and Thingstad,
478 1985). So far, CO_2 enrichment experiments examining natural plankton assemblages (e.g.
479 Engel, et al., 2005; Hopkinson et al., 2010; Riebesell et al., 2007; Bach et al., 2016) did not
480 reveal a consistent pattern of species response or primary production to elevated CO_2 . Spilling
481 et al. (2016a) could not detect any effect of increased CO_2 on total primary production, even
482 though Crawford et al. (2016) reported effects of CO_2 on several groups of
483 picophytoplankton. During our study, although one larger picoeukaryote (Pico III) was
484 negatively impacted by $f\text{CO}_2$, two small picoeukaryotes (Pico I, Pico II) benefitted from the
485 CO_2 addition, yielding significantly higher growth rates and BVs at higher $f\text{CO}_2$ (Crawford et
486 al., 2016). This is consistent with recent evidence suggesting a positive impact of enhanced
487 $f\text{CO}_2$ on the abundance of small picoeukaryotic phytoplankton (Brussaard et al., 2013;
488 Newbold et al., 2012; Endo et al., 2013; Sala et al., 2015, Bach et al., 2016). Both
489 picoeukaryotic groups were identified as variables explaining the separation along the
490 gradient of $f\text{CO}_2$ on the second and third dbRDA-axis in the DistLM ordination of the
491 bacteria-phytoplankton community. Specifically, Pico I was highly negatively correlated ($r_s=-$
492 0.67) to dbRDA axis two. However, dbRDA indicated also opposing effects of $f\text{CO}_2$ on
493 Pico II ($r_s=0.54$) and HDNA prokaryotes ($r_s=-0.31$), being positively or negatively correlated
494 with axis three. Indeed, sharp increases in $\text{BV}_{\text{Pico II}}$ at high $f\text{CO}_2$ between t14-17 were
495 associated with decreases in BV_{HDNA} .

496 Although we are not able to draw conclusions on the interaction of these two particular groups
497 of organisms, a cluster analysis of pairwise Spearman correlations between functional groups
498 of bacteria and phytoplankton revealed a distinct clustering with mesocosms based on $f\text{CO}_2$
499 concentration (Fig. 4). We also detected a change in the ratio of heterotrophic bacterial BV to
500 Chl *a* between the different $f\text{CO}_2$ -treatments, though this change was not visible for the entire

501 study duration and not consistent with $f\text{CO}_2$. These results strongly suggest that trophic
502 interactions between functional groups of bacteria and phytoplankton might be changing in a
503 future acidified ocean.

504 In nutrient poor systems, variable growth rates of phytoplankton, DOM quality and quantity,
505 but also losses of phyto- and bacterioplankton due to grazing or viral lyses may potentially
506 contribute to this observed decoupling of phytoplankton and bacterioplankton at high $f\text{CO}_2$
507 (Azam et al., 1983; Bratbak and Thingstad, 1985; Caron et al., 1988; Sheik et al., 2014). The
508 viral shunt or bacterivory may release phytoplankton from competition with bacteria for
509 limiting nutrients (e.g. Bratbak and Thingstad, 1985; Caron and Goldman, 1990). How
510 increased $f\text{CO}_2$ will affect these processes (e.g. viral lysis and bacterial grazing) under nutrient
511 limited conditions remains so far uncertain. Bacterial grazing by mixotrophs, which would
512 also directly benefit from increased CO_2 availability (Rose et al., 2009), may provide a
513 mechanism for recycling of inorganic nutrients, otherwise bound in bacterial biomass, as a
514 means for supporting phytoplankton growth (Sanders, 1991; Hartmann et al., 2012; Calbet et
515 al., 2012; Mitra et al. 2014). However, other studies examining bacterial grazing under
516 different nutrient conditions reported conflicting positive and negative results of increased
517 $f\text{CO}_2$ (e.g. Brussaard et al., 2013; Rose et al., 2009; Suffrian et al., 2008). Although we are
518 unable to draw defined conclusions on how this myriad of complex biological processes are
519 impacted by $f\text{CO}_2$, it is likely that an impact of these processes is likely and may thus account
520 for a portion of the unexplained variance we observed in our multivariate analyses.

521

522 **5 Conclusion**

523 The use of large-volume mesocosms allowed us to test for multiple $f\text{CO}_2$ -related effects on
524 dynamics of heterotrophic bacterial activity and their biovolume in a near-realistic ecosystem
525 by including trophic interactions from microorganisms up to zooplankton. Complex
526 interactions between various trophic levels, which can only be properly addressed at the scale
527 of whole ecosystems, are important for understanding and predicting $f\text{CO}_2$ -induced effects on
528 aquatic food webs and biogeochemistry in a future, acidified ocean. We examined these
529 impacts in a nutrient-depleted system, which is representative for large parts of the oceans
530 (Moore et al., 2013). Heterotrophic bacterial productivity was, for the most part, tightly
531 coupled to the availability of phytoplankton-derived organic matter. When accounting for

532 temporal development and taking into account trophic interactions using multivariate
533 statistics, changes in nutrient composition, metabolic parameters and bacteria-phytoplankton
534 communities revealed a significant effect of the $f\text{CO}_2$ -treatment. Although not consistent
535 throughout the experiment, differences in the ratio of heterotrophic bacterial BV to Chl *a*
536 during the last half of the experiment suggest that a future ocean will become more
537 autotrophic during low productive periods as a result of altered trophic interactions between
538 functional groups of bacteria and phytoplankton. There is additional support for this
539 conclusion from examining the atmospheric exchange of CO_2 (Spilling et al., 2016b). During
540 the limited time-scale of this study, the observed effects of $f\text{CO}_2$ did not manifest as altered
541 carbon export (Paul et al., 2015). However, over several years, maintained changes in nutrient
542 cycling, as a consequence of a permanent decoupling between bacteria and phytoplankton,
543 may arise and impact the nature of the carbon pump.

544

545 **6 Data availability**

546 The primary production and respiration data can be found in Spilling et al. (2016b; doi:
547 10.1594/PANGAEA.863933). Other variables from the experiment (e.g. total particulate and
548 dissolved nutrients) can be found in Paul et al. (2016; doi:10.1594/PANGAEA.863032).

549 Data of Bacterial Protein Production and bacterial abundances will be available with final
550 publication. A PANGAEA data repository will be created.

551

552 **Acknowledgements**

553 We thank the KOSMOS team and all of the participants in the mesocosm campaign for
554 organisation, maintenance and support during the experiment. In particular, we would like to
555 thank Andrea Ludwig for coordinating the campaign logistics and assistance with CTD
556 operations, the diving team and Allanah Paul for her help in data acquisition. Further we
557 thank the Tvärminne Zoological Station for the opportunity to carry out such a big mesocosm
558 experiment at their research station and technical support on site. Additionally we
559 acknowledge the captain and crew of R/V *ALKOR* for their work transporting, deploying
560 (AL394) and recovering (AL397) the mesocosms. Further we thank the two reviewers for
561 their critical comments to improve this manuscript. The collaborative mesocosm campaign

562 was funded by BMBF projects BIOACID II (FKZ 03F06550) and SOPRAN Phase II (FKZ
563 03F0611). CPDB was financially supported by the Darwin project, the Royal Netherlands
564 Institute for Sea Research (NIOZ), and the EU project MESOAQUA (grant agreement
565 number 228224).

566

567 **References**

568 Agawin, N.S.R., Duarte, C.M., Agusti, S.: Nutrient and temperature control of the
569 contribution of picoplankton to phytoplankton biomass and production, *Limnol. Oceanogr.*,
570 45 (3), 591-600, 2000.

571 Akaike, H.: Information theory and an extension of the maximum likelihood principle. In :
572 Petrov, B.N. and Csake, F. (eds.), *Second International Symposium on Information Theory*,
573 *Akademiai Kiado, Budapest*, 267–281, 1973.

574 Akaike, H.: A new look at the statistical model identification. *IEEE Transactions on*
575 *Automatic Control*, AC-19, 716–723, 1974.

576 Allgaier, M., Riebesell, U., Vogt, M., Thyrraug, R., Grossart, H.-P.: Coupling of
577 heterotrophic bacteria to phytoplankton bloom development at different $p\text{CO}_2$ levels: a
578 mesocosm study, *Biogeosciences*, 5, 1007-1022, 2008.

579 Anderson, M.J.: A new method for non-parametric multivariate analysis of variance, *Austral.*
580 *Ecol.*, 35, 32–46, 2001.

581 Anderson, M.J., Gorley, R.N. and Clarke, K.R.: *PERMANOVA+ for PRIMER: Guide to*
582 *Software and Statistical Methods*, PRIMER-E, Plymouth, UK, 214, 2008.

583 Attermeyer, K., Hornick, T., Kayler, Z.E., Bahr, A., Zwirnmann, E., Grossart, H.-P., Premke,
584 K.: Enhanced bacterial decomposition with increasing addition of autochthonous to
585 allochthonous carbon without any effect on bacterial community composition.
586 *Biogeosciences*, 11 (6): 1479-1489, 2014.

587 Attermeyer, K., Tittel, J., Allgaier, M., Frindte, K., Wurzbacher, C.M., Hilt, S., Kamjunke, N.,
588 Grossart, H.-P.: Effects of light and autochthonous carbon additions on microbial turnover of
589 allochthonous organic carbon and community composition, *Microbial Ecology*, 69 (2): 361-
590 371, 2015.

591 Azam, F.: Microbial Control of Oceanic Carbon Flux: The Plot Thickens, *Science*, 280
592 (5364), 694-696, doi:10.1126/science.280.5364.694, 1998.

593 Azam, F., Fenchel, T., Field, J.G., Gray, J.S., Meyer-Reil, L.A., and Thingstad, F.: The
594 Ecological Role of Water-Column Microbes in the Sea, *Mar. Ecol. Prog. Ser.*, 10, 257-263,
595 1983.

596 Bach, L.T., Taucher, J., Boxhammer, T., Ludwig, A., The Kristineberg KOSMOS
597 Consortium, Achterberg, E.P., Algueró-Muizñiz, M., Anderson, L.G., Bellworthy, J.,
598 Büdenbender, J., Czerny, J., Ericson, Y., Esposito, M., Fischer, M., Haunost, M., Hellemann,
599 D., Horn, H.G., Hornick, T., Meyer, J., Sswat, M., Zark, M., Riebesell, U.: Influence of Ocean
600 Acidification on a Natural Winter-to-Summer Plankton Succession: First Insights from a
601 Long-Term Mesocosm Study Draw Attention to Periods of Low Nutrient Concentrations.
602 *PLoS ONE* 11(8): e0159068, doi:10.1371/journal.pone.0159068, 2016.

603 Badr, E.-S. A., Achterberg, E. P., Tappin, A. D., Hill, S. J., and Braungardt, C. B.:
604 Determination of dissolved organic nitro-gen in natural waters using high-temperature
605 catalytic oxidation, *TrAC-Trend, Anal. Chem.*, 22, 819–827, doi:10.1016/S0165-
606 9936(03)01202-0, 2003.

607 Benjamini, Y., and Hochberg, Y.: Controlling the false discovery rate: a practical and
608 powerful approach to multiple testing. *Journal of the Royal Statistical Society Series B*, 57,
609 289-300, 1995.

610 Berggren, M., Lapierre, J.-F., and del Giorgio, P. A.: Magnitude and regulation of
611 bacterioplankton respiratory quotient across fresh-water environmental gradients, *ISME*
612 *Journal*, 6, 984–993, 2012.

613 Bratbak, G., Thingstad, T.F.: Phytoplankton-bacteria interactions: an apparent paradox?
614 Analysis of a model system with both competition and commensalism. *Mar. Ecol. Prog. Ser.*,
615 25, 23-30, 1985.

616 Brett, M.T., Lubnow, F.S., Villar-Argaiz, M., Müller-Solger, A., and Goldman, C.R.: Nutrient
617 control of bacterioplankton and phytoplankton dynamics, *Aquatic Ecology*, 33, 135-145,
618 1999.

619 Brussaard, C. P. D.: Optimization of procedures for counting viruses by flow cytometry,
620 *Appl. Environ. Microb.*, 70, 1506–1513, doi:10.1128/AEM.70.3.1506-1513.2004, 2004.

621 Brussaard, C.P.C., Noordeloos, A.A.M., Witte, H., Collenteur, M.C.J., Schulz, K.G., Ludwig,
622 A., Riebesell, U.: Arctic microbial community dynamics influenced by elevated CO₂ levels,
623 *Biogeosciences*, 10, 719-731, 2013.

624 Burnham, K.P. and Anderson, D.R.: Multimodel inference: understanding AIC and BIC in
625 model selection, *Soc. Method. Res.*, 33, 261–304, 2004.

626 Calbet, A., Martínez, R.A., Isari, S., Zervoudaki, S., Nejstgaard, J.C., Pitta, P., Sazhin, A.F.,
627 Sousoni, D., Gomes, A., Berger, S.A., Tsagaraki, T.M., Pacnik, R.: Effects of light
628 availability on mixotrophy and microzooplankton grazing in an oligotrophic plankton food
629 web: Evidences from a mesocosm study in Eastern Mediterranean waters, *Journal of*
630 *Experimental Marine Biology and Ecology*, 424-425, 66-77, 2012.

631 Caldeira, K. and Wickett, M.E.: Anthropogenic carbon and ocean pH, *Nature*, 425, 365, 2003.

632 Caron, D.A., Goldman, J.C.: Protozoan nutrient regeneration. In: Capriulo GM (Ed.) *Ecology*
633 *of marine protozoa*, Oxford University Press, New York, p 283–306, 1990.

634 Caron, D.A., Goldman, J.C., Dennett, M.R.: Experimental demonstration of the roles of
635 bacteria and bacterivorous protozoa in plankton nutrient cycles, *Hydrobiologia*, 159, 27-40,
636 1988.

637 Cauwet, G., Déliat, G., Krastev, A., Shtereva, G., Becqueevort, S., Lancelot, C., Momzikoff,
638 A., Saliot, A., Cociasu, A., Popa, L.: Seasonal DOC accumulation in the Black Sea: a regional
639 explanation for a general mechanism, *Marine Chemistry*, 79, 193-205, 2002.

640 Cho, B.C., Azam, F.: Major role of bacteria in biogeochemical fluxes in the ocean's interior,
641 *Nature*, 332, 441-443, 1988.

642 Clarke, K.R. and Gorley, R.N.: *PRIMER v5: User manual/tutorial*, Plymouth, UKPRIMER-E,
643 91 pp., 2001.

644 Clarke, K.R. and Gorley, R.N.: *PRIMER v6: User manual/tutorial*, PRIMER-E, Plymouth,
645 UK, 115 pp., 2006.

646 Clarke, K.R. and Green, R.H.: Statistical design and analysis for a 'biological effects' study.
647 *Mar. Ecol. Prog. Ser.*, 46, 213–226, 1988.

648 Crawford, K.J., Riebesell, U., and Brussaard, C.P.D.: Shifts in the microbial community in the
649 Baltic Sea with increasing CO₂, *Biogeosciences Discuss.*, doi:10.5194/bg-2015-606, in
650 review, 2016.

651 de Kluijver, A., Soetaert, K., Schultz, K.-G., Riebesell, U., Bellerby, R.G.J, and Middelburg,
652 J.J.: Phytoplankton-bacteria coupling under elevated CO₂ levels: a stable isotope labelling
653 study, *Biogeosciences*, 7, 3783-3793, 2010.

654 Dickson, A.G., Sabine, C., and Christian, J. (Eds.): Guide to best practices for ocean CO₂
655 measurements, PICES Special Publication 3, 191 pp., <http://aquaticcommons.org/1443/> (last
656 access: 16 October 2012), 2007.

657 Drakare, S., Blomqvist, P., Bergström, A.-K. and Jansson, M.: Relationships between
658 picophytoplankton and environmental variables in lakes along a gradient of water colour and
659 nutrient content, *Freshwater Biology*, 48, 729-740, 2003.

660 Egge, J.K., Thingstad, T.F., Larsen, A., Engel, A., Wohlers, J., Bellerby, R.G.J., Riebesell, U.:
661 Primary production during nutrient-induced blooms at elevated CO₂ concentrations,
662 *Biogeosciences*, 6, 877-885, 2009.

663 Endo, H., Yoshimura, T., Kataoka, T., Suzuki, K.: Effects of CO₂ and iron availability on
664 phytoplankton and eubacterial community compositions in the northwest subarctic Pacific, *J.*
665 *Exp. Mar. Biol. Ecol.*, 439, 160-175, doi: 10.1016/j.jembe.2012.11.003, 2013.

666 Engel, A., Zondervan, I., Aerts, K., Beaufort, L., Benthien, A., Chou, L., Delille, B., Gattuso,
667 J.-P., Harlay, J., and Heemann, C.: Testing the direct effect of CO₂ concentration on a bloom
668 of the coccolithophorid *Emiliana huxleyi* in mesocosm experiments, *Limnol. Oceanogr.*, 50,
669 493–507, doi:10.4319/lc.2005.50.2.0493, 2005.

670 Fabry, V.J., Seibel, B.A., Feely, R.A., Orr, J.C.: Impacts of ocean acidification on marine
671 fauna and ecosystem processes, *ICES Journal of Marine Science*, 65, 414-432, 2008

672 Gargas, E.: A manual for phytoplankton primary production studies in the Baltic, *The Baltic*
673 *Marine Biologist*, Hørsholm, Denmark, 88 pp., 1975.

674 Grasshoff, K., Ehrhardt, M., Kremling, K., and Almgren, T.: Methods of seawater analysis,
675 Wiley Verlag Chemie GmbH, Weinheim, Germany, 1983.

676 Grossart, H.-P.: Ecological consequences of bacterioplankton lifestyles: changes in concepts
677 are needed. *Environ. Microbiol. Rep.*, 2, 706–714. doi: 10.1111/j.1758-2229.2010.00179.x,
678 2010.

679 Grossart, H.-P. and Simon, M.: Limnetic macroscopic organic aggregates (lake snow):
680 Occurrence, characteristics, and microbial dynamics in Lake Constance, *Limnol. Oceanogr.*,
681 38, 532-546, 1993.

682 Grossart H.-P., Hietanen S., Ploug H.: Microbial dynamics on diatom aggregates in Øresund,
683 Denmark. *Marine Ecology Progress Series*, 249: 69-78, 2003.

684 Grossart, H.-P., Allgaier, M., Passow, U., Riebesell, U.: Testing the effect of CO₂
685 concentration on the dynamics of marine heterotrophic bacterioplankton, *Limnology and*
686 *Oceanography*, 51, 1-11, 2006a

687 Grossart, H.-P., Czub, G., and Simon, M.: Specific interactions of planktonic algae and
688 bacteria: Implications for aggregation and organic matter cycling in the sea, *Environ.*
689 *Microbiol.*, 8, 1074–1084, 2006b.

690 Hagström, Å., Larsson, U., Hörstedt, P., Normark, S.: Frequency of Dividing Cells, a New
691 Approach to the Determination of Bacterial Growth Rates in Aquatic Environments, *Appl.*
692 *Environ. Microbiol.*, 37 (5), 805-812, 1979.

693 Hansen, H. P. and Koroleff, F.: Determination of nutrients, in *Methods of Seawater Analysis*,
694 edited by: Grasshoff, K., Kremling, K., and Ehrhardt, M., Wiley Verlag Chemie GmbH,
695 Zeinheim, Germany, 159–228, 1999.

696 Harrell, F.E. Jr., with contributions from Dupont, C. and many others: Hmisc: Harrell
697 Miscellaneous. R package version 3.17-4, [http:// CRAN.R-project.org/package=Hmisc](http://CRAN.R-project.org/package=Hmisc),
698 2016.

699 Hartmann, M., Grob, C., Tarran, G.A., Martin, A.P., Burkill, P.H., Scanlan, D.J. and Zubkov,
700 M.V.: Mixotrophic basis of Atlantic oligotrophic ecosystems, *Proc. Natl. Acad. Sci. U.S.A.*,
701 109 (15), 5756-5760, doi:10.1073/pnas.1118179109, 2012.

702 Hein, M. and Sand-Jensen, K.: CO₂ increases oceanic primary production, *Nature*, 388, 526-
703 527, doi:10.1038/41457, 1997.

704 Hobbie, J.E., Daley, R.J., Jasper, S.: Use of nuclepore filters for counting bacteria by
705 fluorescence microscopy, *Appl. Environ. Microbiol.*, 33, 1225-1228, 1977.

706 Hoikkala, L., Aarnos, H., Lignell, R.: Changes in Nutrient and Carbon Availability and
707 Temperature as Factors Controlling Bacterial Growth in the Northern Baltic Sea., *Estuaries
708 and Coasts*, 32, 720-733, doi:10.1007/s12237-009-9154-z, 2009.

709 Hopkinson, B. M., Xu, Y., Shi, D., McGinn, P. J., and Morel, F. M. M.: The effect of CO₂ on
710 the photosynthetic physiology of phytoplankton in the Gulf of Alaska, *Limnol. Oceanogr.*, 55,
711 2011–2024, doi:10.4319/lo.2010.55.5.2011, 2010.

712 Joint, I., Henriksen, P., Fonnes, G.A., Bourne, D., Thingstad, T.F., Riemann, B.: Competition
713 for inorganic nutrients between phytoplankton and bacterioplankton in nutrient manipulated
714 mesocosms, *Aquat. Microb. Ecol.*, 29, 145-159, 2002.

715 Karner, M.B., DeLong, E.F. and Karl, D.M.: Archaeal dominance in the mesopelagic zone of
716 the Pacific Ocean, *Nature*, 409, 507-510, 2001.

717 Kirchman, D.L.: The Uptake of Inorganic Nutrients by Heterotrophic Bacteria, *Microb. Ecol.*,
718 28, 255-271, 1994

719 Kirchman, D.L., Elifantz, H., Dittel, A.I., Malmstrom, R.R. and Cottrell, M.T.: Standing
720 stocks and activity of Archaea and Bacteria in the western Arctic Ocean, *Limnol. Oceanogr.*,
721 52 (2), 495-507, 2007.

722 Kivi, K., Kaitala, S., Kuosa, H., Kuparinen, J., Leskinen, E., Lignell, R., Marcussen, B. and
723 Tamminen, T.: Nutrient limitation and grazing control of the Baltic plankton community
724 during annual succession. *Limnology and Oceanography* 38: 893–905, 1993.

725 Kuparinen, J. and Heinänen, A.: Inorganic Nutrient and Carbon Controlled Bacterioplankton
726 Growth in the Baltic Sea. *Estuarine, Coastal and Shelf Science* 37: 271–285, 1993.

727 Lapoussière, A., Michel, C., Starr, M., Gosselin, M., Poulin, M.: Role of free-living and
728 particle-attached bacteria in the recycling and export of organic material in the Hudson Bay
729 system, *Journal of Marine Systems*, 88, 434-445, 2011.

730 Legendre, P. and Anderson, M.J.: Distance-based redundancy analysis: testing multispecies
731 responses in multifactorial ecological experiments. *Ecol. Monogr.*, 69, 1–24, 1999.

732 Lignell, R., Hoikkala, L., Lahtinen, T.: Effects of inorganic nutrients, glucose and solar
733 radiation treatments on bacterial growth and exploitation of dissolved organic carbon and
734 nitrogen in the northern Baltic Sea. *Aquat. Microb. Ecol.*, 51, 209–221, 2008.

735 Lindh, M.V., Riemann, L., Balter, F., Romero-Oliva, C., Salomon, P.S., Graneli, E. and
736 Pinhassi, J.: Consequences of increased temperature and acidification on bacterioplankton
737 community composition during a mesocosm spring bloom in the Baltic Sea, *Environmental*
738 *Microbiology Reports*, 5, 252-262, 2013.

739 Losh, J.L., Morel, F.M.M., Hopkinson, B.M.: Modest increase in the C:N ratio of N-limited
740 phytoplankton in the California Current in response to high CO₂, *Mar. Ecol.-Prog. Ser.*, 468,
741 31-42, doi:10.3354/meps09981, 2012.

742 Lueker, T.J., Dickson, A.G., and Keeling, C.D.: Ocean pCO₂ calculated from dissolved
743 inorganic carbon, alkalinity, and equations for K₁ and K₂: validation based on laboratory
744 measurements of CO₂ in gas and seawater at equilibrium, *Mar. Chem.*, 70, 105-119,
745 doi:10.1016/S0304-4203(00)00022-0, 2000.

746 Maat, D.S., Crawford, K.J., Timmermans, K.R. and Brussaard, C.P.D.: Elevated CO₂ and
747 Phosphate Limitation Favor *Micromonas pusilla* through Stimulated Growth and Reduced
748 Viral Impact, *Appl. Environ. Microbiol.*, 80 (10), 3119-3127, doi:10.1128/AEM.03639-13,
749 2014.

750 Mardia, K.V., Kent, J.T., and Bibby, J.M.: *Multivariate Analysis*, London: Academic Press,
751 1979.

752 Marie, D., Brussaard, C.P.D., Thyrrhaug, R., Bratbak, G., Vaultot, D.: Enumeration of marine
753 viruses in culture and natural samples by flow cytometry, *Appl. Environ. Microbiol.*, 65(1),
754 45-52, 1999.

755 Massana, R., Gasol, J.M., Bjørnsen, P.K., Blackburn, N., Hagström, Å, Hietanen, S., Hygum,
756 B.H., Kuparinen and Pedrós-Alió C.: Measurement of bacterial size via image analysis of
757 epifluorescence preparations: description of an inexpensive system and solutions to some of
758 the most common problems, *Sci. Mar.*, 61(3), 397-407, 1997.

759 Mauriac, R., Moutin, T., Baklouti, M.: Accumulation of DOC in Low Phosphate Low
760 Chlorophyll (LPLC) area: is it related to higher production under high N:P ratio?,
761 *Biogeosciences*, 8, 933-950, 2011.

762 McArdle, B.H. and Anderson, M.J.: Fitting multivariate models to community data: A
763 comment on distance-based redundancy analysis, *Ecology*, 82 (1), 290–297, 2001.

764 Mehrbach, C., Culberson, C.H., Hawley, J.E., and Pytkowicz, R.M.: Measurement of apparent
765 dissociation constants of carbonic acid in seawater at atmospheric pressure, *Limnol.*
766 *Oceanogr.*, 18, 897-807, 1973.

767 Mitra, A., Flynn, K.J., Burkholder, J.M., Berge, T., Calbet, A., Raven, J.A., Granéli, E.,
768 Gilbert, P.M., Hansen, P.J., Stoecker, D.K., Thingstad, F., Tillmann, U., Våge, S., Wilken, S.,
769 and Zubkov, M.V.: The role of mixotrophic protists in the biological carbon pump,
770 *Biogeosciences*, 11, 995-1005, doi:10.5194/bg-11-995-2014, 2014.

771 Mojica, K. D. A., Evans, C., and Brussaard, C. P. D.: Flow cytometric enumeration of marine
772 viral populations at low abundances, *Aquat. Microb. Ecol.*, 71, 203–209,
773 doi:10.3354/ame01672, 2014.

774 Moore, C.M., Mills, M.M., Arrigo, K.R., Berman-Frank, I, Bopp, L., Boyd, P.W., Galbraith,
775 E.D., Geider, R.J., Guieu, C., Jaccard, S.L., Jickells, T.D., La Roche, J., Lenton, T.M.,
776 Mahowald, N.M., Marañón, E., Marinov, I., Moore, J.K., Nakatsuka, T., Oschlies, A., Sito,
777 M.A., Thingstad, T.F., Tsuda, A. and Ulloa, O.: Processes and patterns of oceanic nutrient
778 limitation, *Nature Geoscience*, 6(9), 701-710, doi:10.1038/NGEO1765, 2013.

779 Mosley, L.M., Husheer, S.L.G., and Hunter, K.A.: Spectrophotometric pH measurement in
780 estuaries using thymol blue and *m*-cresol purple, *Mar. Chem.*, 91, 175-186,
781 doi:10.1016/j.marchem.2004.06.008, 2004.

782 Nausch, M., Bach, L.T., Czerny, J., Godstein, J., Grossart, H.-P., Hellemann, D., Hornick, T.,
783 Achterberg, E.P., Schulz, K.-G., and Riebesell, U.: Effects of CO₂ perturbation on phosphorus
784 pool sizes and uptake in a mesocosm experiment during a low productive summer season in
785 the northern Baltic Sea, *Biogeosciences*, 13, 3035-3050, doi:10.5194/bg-13-3035-2016, 2016.

786 Newbold, L., Oliver, A.E., Booth, T., Tiwari, B., DeSantis, T., Maguire, M., Andersen, G.,
787 van der Gast, C.J., and Whiteley, A.S.: The response of marine picoplankton to ocean
788 acidification, *Environmental Microbiology*, 14 (9), 2293-2307, 2012.

789 Oksanen, J., Blanchet, F.G., Friendly, M., Kindt, R., Legendre, P., McGlenn, D., Minchin,
790 P.R., O'Hara, R.B., Simpson, G.L., Solymos, P., Stevens, M.H.H., Szoecs, E., and Wagner,

791 H.: vegan: Community Ecology Package. R package version 2.4-0, [https://CRAN.R-](https://CRAN.R-project.org/package=vegan)
792 [project.org/package=vegan](https://CRAN.R-project.org/package=vegan), 2016.

793 Patey, M. D., Rijkenberg, M. J. A., Statham, P. J., Stinchcombe, M. C., Achterberg, E. P., and
794 Mowlem, M.: Determination of nitrate and phosphate in seawater at nanomolar
795 concentrations, *TrAC-Trend, Anal. Chem.*, 27, 169–182, doi:10.1016/j.trac.2007.12.006,
796 2008.

797 Paul, A.J., Bach, L.T., Schulz, K.-G., Boxhammer, T., Czerny, J., Achterberg, E.P.,
798 Hellemann, D., Trense, Y., Nausch, M., Sswat, M., Riebesell, U.: Effect of elevated CO₂ on
799 organic matter pools and fluxes in a summer Baltic Sea plankton community, *Biogeosciences*,
800 12, 1-23, doi:10.5194/bg-12-1-2015, 2015.

801 Platt, T., Rao, D.V.S., Irwin, B.: Photosynthesis of picoplankton in the oligotrophic ocean,
802 *Nature*, 301, 702-704, 1983.

803 Porter, K.G., Feig, Y.S.: Dapi for identifying and counting aquatic microflora, *Limnol.*
804 *Oceanogr.*, 25, 943-948, 1980.

805 Raven, J.A.: The twelfth Tansley Lecture. Small is beautiful: the picophytoplankton,
806 *Functional Ecology*, 12, 503-513, 1998.

807 Raven, J., Caldeira, K., Elderfield, H., Hoegh-Guldberg, O., Liss, P., Riebesell, U.,
808 Shepherd, J., Turley, C., Watson, A.: *Ocean Acidification due to Increasing Atmospheric*
809 *Carbon Dioxide*, The Royal Society, London, UK, 2005.

810 R Core Team (2016). *R: A language and environment for statistical computing*. R Foundation
811 for Statistical Computing, Vienna, Austria, URL <http://www.R-project.org/>, 2014.

812 Riebesell, U., Gattuso, J.-P.: Lessons learned from ocean acidification research. Reflection on
813 the rapidly growing field of ocean acidification research highlights priorities for future
814 research on the changing ocean. *Nature Climate Change*, 5, 12-14, doi:10.1038/nclimate2456,
815 2015.

816 Riebesell, U., Schulz, K.G., Bellerby, R.G.J., Botros, M., Fritsche, P., Meyerhöfer, M., Neill,
817 C., Nondal, G., Oschlies, A., Wohlers and J., Zöllner, E.: Enhanced biological carbon
818 consumption in a high CO₂ ocean, *Nature Letters*, 450 (22), 545-548,
819 doi:10.1038/nature06267, 2007.

820 Riebesell, U., Czerny, J., von Bröckel, K., Boxhammer, T., Büdenbender, J., Deckelnick, M.,
821 Fischer, M., Hoffmann, D., Krug, S.A., Lentz, U., Ludwig, A., Mucbe, and Schluz, K.G.:
822 Technical Note: A mobile sea-going mesocosm system – new opportunities for ocean change
823 research, *Biogeosciences*, 10, 1835-1847, doi:10.5194/bg-10-1835-2013, 2013a.

824 Riebesell, U., Gattuso, J.-P., Thingstad, T.F. and Middelburg, J.J.: Arctic ocean acidification:
825 pelagic ecosystem and biogeochemical responses during a mesocosm study, *Biogeosciences*,
826 10, 5619-5626, doi:10.5194/bg-10-5619-2013, 2013b.

827 Rieck, A., Herlemann, D.P.R., Jürgens, K. and Grossart, H.-P.: Particle-Associated Differ
828 from Free-Living Bacteria in Surface Waters of the Baltic Sea, *Front. Microbiol.*, 6 (1297),
829 doi:10.3389/fmicb.2015.01297, 2015.

830 Rose, J.M., Feng, Y., Gobler, C.J., Gutierrez, R., Hare, C.E., Leblanc, K., Hutchins, D.A.:
831 Effects of increased pCO₂ and temperature on the North Atlantic spring bloom. II.
832 Microzooplankton abundance and grazing, *Mar. Ecol. Prog. Ser.*, 388, 27-40, 2009.

833 Rösel, S., Grossart, H.-P.: Contrasting dynamics in activity and community composition of
834 free-living and particle-associated bacteria in spring, *Aquatic Microbial Ecology*, 66 (1), 169-
835 181, 2012.

836 Sabine, C. L., Feely, R. A., Gruber, N., Key, R. M., Lee, K., Bullister, J. L., Wanninkhof,
837 R., Wong, C. S., Wallace, D.W., Tilbrook, B., Millero, F. J., Peng, T. H., Kozyr, A., Ono, T.,
838 and Rios, A. F.: The oceanic sink for anthropogenic CO₂, *Science*, 305, 367–371, 2004.

839 Sala, M.M., Aparicio, F.L., Balagué, V., Boras, A., Borrull, E., Cardelús, C., Cros, L., Gomes,
840 A., López-Sanz, A., Malits, A., Martinez, R.A., Mestre, M., Movilla, J., Sarmiento, H.,
841 Vázquez-Dominguez, E., Vaqué, D., Pinhassi, J., Calbet, A., Calvo, E., Gasol, J.M., Pelejero,
842 C., Marrasé, C.: Contrasting effects of ocean acidification on the microbial food web under
843 different trophic conditions, *ICES Journal of Marine Science*, doi:10.1093/icesjms/fsv130,
844 2015.

845 Sanders, R.W.: Mixotrophic Protists in Marine and Freshwater Ecosystems, *J. Protozool.*, 38
846 (1), 76-81, 1991.

847 Sharp, J.: Improved analysis for particulate organic carbon and nitrogen from seawater,
848 *Limnol. Oceanogr.*, 19, 984–989, 1974.

849 Sheik, A.R., Brussaard, C.P.D., Lavik, G., Lam, P., Musat, N., Krupke, A., Littmann, S.,
850 Strous, M. and Kuypers M.M.M.: Responses of the coastal bacterial community to viral
851 infection of the algae *Phaeocystis globosa*, *The ISME Journal*, 8, 212-225, doi:
852 10.1038/ismej.2013.135, 2014.

853 Simon, M., Azam, F.: Protein content and protein synthesis rates of planktonic marine
854 bacteria, *Marine Ecology Progress Series*, 51, 201-213, 1989.

855 Simon, M., Grossart, H.-P., Schweitzer, B., and Ploug, H.; Microbial ecology of organic
856 aggregates in aquatic ecosystems. *Aquat. Microb. Ecol.*, 28, 175–211,
857 doi:10.3354/ame028175, 2002.

858 Smith, D.C., Simon, M., Alldredge, A.L., Azam, F.: Intense hydrolytic enzyme activity on
859 marine aggregates and implications for rapid particle dissolution, *Nature*, 359, 139-142, 1992.

860 Søndergaard, M., Williams, P. le B., Cauwet, G., Riemann, B., Rabinson, C., Terzic, S.,
861 Woodward, E.M.S., Worm, J.: Net accumulation and flux of dissolved organic carbon and
862 dissolved organic nitrogen in marine plankton communities, *Limnol. Oceanogr.*, 45(5), 1097-
863 1111, 2000.

864 Spilling, K., Paul, A.J., Virkkala, N., Hastings, T., Lischka, S., Stuhr, A., Bermudéz, R.,
865 Czerny, J., Boxhammer, T., Schulz, K.G., Ludwig, A., and Riebesell, U.: Ocean acidification
866 decreases plankton respiration: evidence from a mesocosm experiment, *Biogeosciences*, 13,
867 4707-4719, doi:10.5194/bg-13-4707-2016, 2016a.

868 Spilling, K., Schulz, K. G., Paul, A. J., Boxhammer, T., Achterberg, E. P., Hornick, T.,
869 Lischka, S., Stuhr, A., Bermúdez, R., Czerny, J., Crawford, K.J., Brussaard, C. P. D.,
870 Grossart, H.-P., and Riebesell, U.: Effects of ocean acidification on pelagic carbon fluxes in a
871 mesocosm experiment, *Biogeosciences Discuss.*, doi:10.5194/bg-2016-56, in review, 2016b.

872 Steeman-Nielsen, E.: The use of radioactive carbon for measuring organic production in the
873 sea, *J. Cons. Int. Explor. Mer.*, 18, 117–140, 1952.

874 Suffrian, K., Simonelli, P., Nejstgaard, J.C., Putzeys, S., Carotenuto, Y., and Antia, A.N.:
875 Microzooplankton grazing and phytoplankton growth in marine mesocosms with increased
876 CO₂ levels. *Biogeosciences*, 5, 1145-1156, 2008.

877 Suttle, C.A., Fuhrman, J.A., Capone, D.G.: Rapid ammonium cycling and concentration-
878 dependent partitioning of ammonium and phosphate: Implications for carbon transfer in
879 planktonic communities, *Limnol. Oceanogr.*, 35 (2), 424-433, 1990.

880 Suzuki, R., Shimodaira, H.: pvclust: Hierarchical Clustering with p-values via Multiscale
881 Bootstrap Resampling, R package version 2.0-0., [https://CRAN.R-](https://CRAN.R-project.org/package=pvclust)
882 [project.org/package=pvclust](https://CRAN.R-project.org/package=pvclust), 2015.

883 Taylor, A.R., Brownlee, C., Wheeler, G.L.: Proton channels in algae: reasons to be excited,
884 *Trends in Plant Sciences*, 17(11), 675-684, doi:10.1016/j.tplants.2012.06.009, 2012

885 Thingstad, T.F., and R. Lignell, R.: Theoretical models for the control of bacterial growth
886 rate, abundance, diversity and carbon demand. *Aquat. Microb. Ecol.*, 13, 19–27, 1997.

887 Thingstad, T.F., Hagström, Å., Rassoulzadegan, F.: Accumulation of degradable DOC in
888 surface waters: It is caused by a malfunctioning microbial loop?, *Limnol. Oceanogr.*, 42(2),
889 398-404, 1997.

890 Thingstad, T.F., Bellerby, R.G.J., Bratbak, G., Borsheim, K.Y., Egge, J.K., Heldal, M.,
891 Larsen, A., Neill, C., Nejstgaard, J., Norland, S., Sandaa, R.-A., Skjoldal, E.F., Tanaka, T.,
892 Thyrhaug, R., Töpper, B.: Counterintuitive carbon-to-nutrient coupling in an Arctic pelagic
893 ecosystem, *Nature Letters*, 455, 387-391, doi:10.1038/nature07235, 2008.

894 Toggweiler, J.R.: Carbon overconsumption, *Nature*, 363, 210-211, 1993.

895 Turley, C.M., Mackie, P.J.: Biogeochemical significance of attached and free-living bacteria
896 and the flux of particles in the NE Atlantic Ocean., *Mar. Ecol. Prog. Ser.*, 115; 191-203, 1994.

897 Venables, W.N., and Ripley, B.D.: *Modern Applied Statistics with S*, Springer-Verlag,
898 2002.

899 Warnes, G.R., Bolker, B., Bonebakker, L., Gentleman, R., Liaw, W.H.A., Lumley, T.,
900 Maechler, M., Magnusson, A., Moeller, S., Schwartz, M., and Venables, B.: gplots: Various R
901 Programming Tools for Plotting Data. R package version 3.0.1, [https://CRAN.R-](https://CRAN.R-project.org/package=gplots)
902 [project.org/package=gplots](https://CRAN.R-project.org/package=gplots), 2016.

903 Welschmeyer, N. A.: Fluorometric analysis of chlorophyll a in the presence of chlorophyll b
904 and pheopigments, *Limnol. Oceanogr.*, 39, 1985–1992, doi:10.4319/lo.1994.39.8.1985, 1994.

905 Wickham, H.: *ggplot2: Elegant graphics for data analysis*. Springer-Verlag New York, 2009.

906 Zhang, J.-Z. and Chi, J.: Automated analysis of nanomolar concentrations of phosphate in
907 natural waters with liquid waveguide, *Environ. Sci. Technol.*, 36, 1048–1053,
908 doi:10.1021/es011094v, 2002.

909 Zweifel, U.L., Norrman, B., and Hagström, Å.: Consumption of dissolved organic carbon by
910 marine bacteria and demands for inorganic nutrients. *Marine Ecology Progress Series* 101,
911 23–32, 1993.

1 Table 1: Results of two-factor permutational multivariate analysis of variance
 2 (PERMANOVA)^(*) on a resemblance matrix (Euclidian distance) of normalized chemical
 3 variables (Phosphate, DOC, TDN, DSi, TPC, PON, POP, PBsi). Time (Ti); *f*CO₂-treatment
 4 (*f*CO₂); Residuals (Res).

Source of variation	<i>df</i>	SS	MS	Pseudo-<i>F</i>	<i>p</i> (<i>perm</i>)	Unique perms
Time	9	309.93	34.436	11.118	0.0001	9920
<i>f</i>CO₂^(**)	4	31.974	7.9936	2.5808	0.0246	9936
Time x <i>f</i>CO₂	36	80.177	2.2271	0.71906	0.8794	9904
Res	10	30.973	3.0973			
Total	59	472				

5 ^(*) Permutation was performed with unrestricted permutation of raw data.

6 ^(**) Pair-wise test could only be performed for control-mesocosms (n=2) with each *f*CO₂-treatment (n=1), due to
 7 missing replication for each *f*CO₂-treatment. Pair-wise comparison was only significant between control and the
 8 highest *f*CO₂-treatment (*p*_{perm}=0.029).

9
 10
 11
 12
 13
 14
 15
 16
 17
 18
 19
 20
 21
 22

1 Table 2: Eigenvectors and -values of the first four axes of a PCA on normalized variables of
 2 dissolved and particulate nutrients. Ordination of the PCA is visualized in Fig. 6.

Variable	PC1	PC2	PC3	PC4
DOC	-0.4	-0.23	0.04	0.68
TDN	0.39	0.21	0.21	0.47
Phosphate	-0.1	0.48	-0.74	0.35
DSi	0.3	0.52	-0.03	-0.24
TPC	0.48	-0.06	0.03	0.13
PON	0.46	-0.05	-0.05	0.16
POP	0.36	-0.39	-0.04	0.21
PBsi	0.17	-0.51	-0.63	-0.22
% variation	49.2	19.7	11.4	7.2
cum. % variation	49.2	68.9	80.4	87.6

3
 4
 5
 6
 7
 8
 9
 10
 11
 12
 13
 14
 15
 16
 17

1 Table 3: Results of two-factor permutational multivariate analysis of variance
 2 (PERMANOVA)^(*) on a resemblance matrix (Euclidian distance) based on normalized
 3 metabolic variables (bacterial protein production (BPP), areal primary production (PP) and
 4 community respiration (CR)). Time (Ti); *f*CO₂-treatment (*f*CO₂); Residuals (Res).

Source of variation	<i>df</i>	SS	MS	Pseudo-<i>F</i>	<i>p</i> (<i>perm</i>)	Unique perms
Time	9	92.128	10.236	6.73	0.001	9931
<i>f</i>CO₂^(**)	4	16.044	4.011	2.637	0.023	9944
Time x <i>f</i>CO₂	36	42.721	1.1867	0.78018	0.792	9904
Res	10	15.21	1.521			
Total	59	182.46				

5 ^(*) Permutation was performed with unrestricted permutation of raw data.

6 ^(**) Pair-wise test could only be performed for control-mesocosms (n=2) with each *f*CO₂-treatment (n=1), due to
 7 missing replication for each *f*CO₂-treatment. Pair-wise comparisons were significant between control and all
 8 *f*CO₂-treatments (*p*_{perm}<0.04).

9

10

11

12

13

14

15

16

17

18

19

20

21

22

23

1 Table 4: Summary of a DistLM procedure for modelling the relationship between
 2 physicochemical variables and a resemblance matrix based on a multivariate assemblage
 3 comprising normalized data of bacterial protein production (BPP), areal primary production
 4 (PP) and community respiration (CR). Non-redundant physicochemical variables were
 5 removed prior analysis. Therefore PON and pH were excluded from the subsequent analysis
 6 due to high correlations ($r_s > 0.9$) to TPC and $f\text{CO}_2$, respectively.

Variable	SS (trace)	Pseudo- <i>F</i>	<i>p</i>	Prop.
<i>f</i> CO ₂	5.0551	1.6527	0.1759	0.03
Temp ^(*)	10.209	3.4376	0.0229	0.055
PAR ^(*)	6.2466	2.056	0.1067	0.034
DOC ^(*)	8.6228	2.8769	0.0474	0.047
TDN	4.7628	1.5545	0.1984	0.026
Phosphate ^(*)	12.319	4.1994	0.0111	0.068
DSi	0.26167	0.083	0.9648	0.001
TPC	7.7827	2.5842	0.0613	0.004
POP	5.0171	1.6399	0.1818	0.027
PBsi	11.688	3.9696	0.0111	0.064

7 ^(*) variables selected in step-wise procedure based on AIC.

8
 9
 10
 11
 12
 13
 14
 15
 16
 17
 18

1 Table 5: Results of two-factor permutational multivariate analysis of variance
 2 (PERMANOVA)^(*) on a resemblance matrix (Bray Curtis similarity) based on log(X+1)
 3 transformed abundances of Pico I-III, Nano I-II, FL bacteria (HDNA, LDNA), PA bacteria,
 4 Cyanobacteria and Chl *a*. Time (Ti); *f*CO₂-treatment (*f*CO₂); Residuals (Res).

Source of variation	<i>df</i>	SS	MS	Pseudo-<i>F</i>	<i>p</i> (<i>perm</i>)	Unique perms
Time	9	201.83	22.426	56.754	0.0001	9923
<i>f</i>CO₂^(**)	4	23.631	5.9077	14.951	0.0001	9940
Time x <i>f</i>CO₂	36	19.859	0.55164	1.396	0.151	9915
Res	10	3.9515	0.39515			
Total	59	271.01				

5 ^(*) Permutation was performed with unrestricted permutation of raw data.

6 ^(**) Pair-wise test could only be performed for control-mesocosms (n=2) with each *f*CO₂-treatment (n=1), due to
 7 missing replication for each *f*CO₂-treatment. Pair-wise comparisons were significant between control and all
 8 *f*CO₂-treatments (*p*_{perm}<0.01).

9
 10
 11
 12
 13
 14
 15
 16
 17
 18
 19
 20
 21
 22
 23

1 Table 6: Summary of a DistLM procedure for modelling the relationship between
 2 physicochemical variables and a multivariate assemblage comprising variables of the bacterial
 3 and phytoplankton community. The resemblance matrix (Bray Curtis similarity) was based on
 4 $\log(X+1)$ transformed abundances of Pico I-III, Nano I-II, FL bacteria (HDNA, LDNA), PA
 5 bacteria, *Synechococcus* spp. and Chl *a*. Non-redundant physicochemical variables were
 6 removed prior analysis. Therefore PON and pH were excluded from the subsequent analysis
 7 due to high correlations ($r_s > 0.9$) to TPC and $f\text{CO}_2$, respectively.

Variable	SS (trace)	Pseudo- <i>F</i>	<i>p</i>	Prop.
<i>f</i> CO ₂ ^(*)	20.469	4.7386	0.0119	0.075
Temp ^(*)	51.838	13.718	0.0001	0.191
PAR	10.791	2.4051	0.0813	0.039
DOC	11.14	2.4864	0.0769	0.041
TDN	9.4456	2.0945	0.1078	0.034
Phosphate ^(*)	25.649	6.063	0.0029	0.095
DSi	9.5766	2.1246	0.103	0.035
TPC ^(*)	36.038	8.8955	0.0002	0.133
POP	52.171	13.827	0.0001	0.193
PBsi	36.439	9.01	0.0005	0.134

8 ^(*) variables selected in step-wise procedure based on AIC.

9
 10
 11
 12
 13
 14
 15
 16
 17
 18
 19

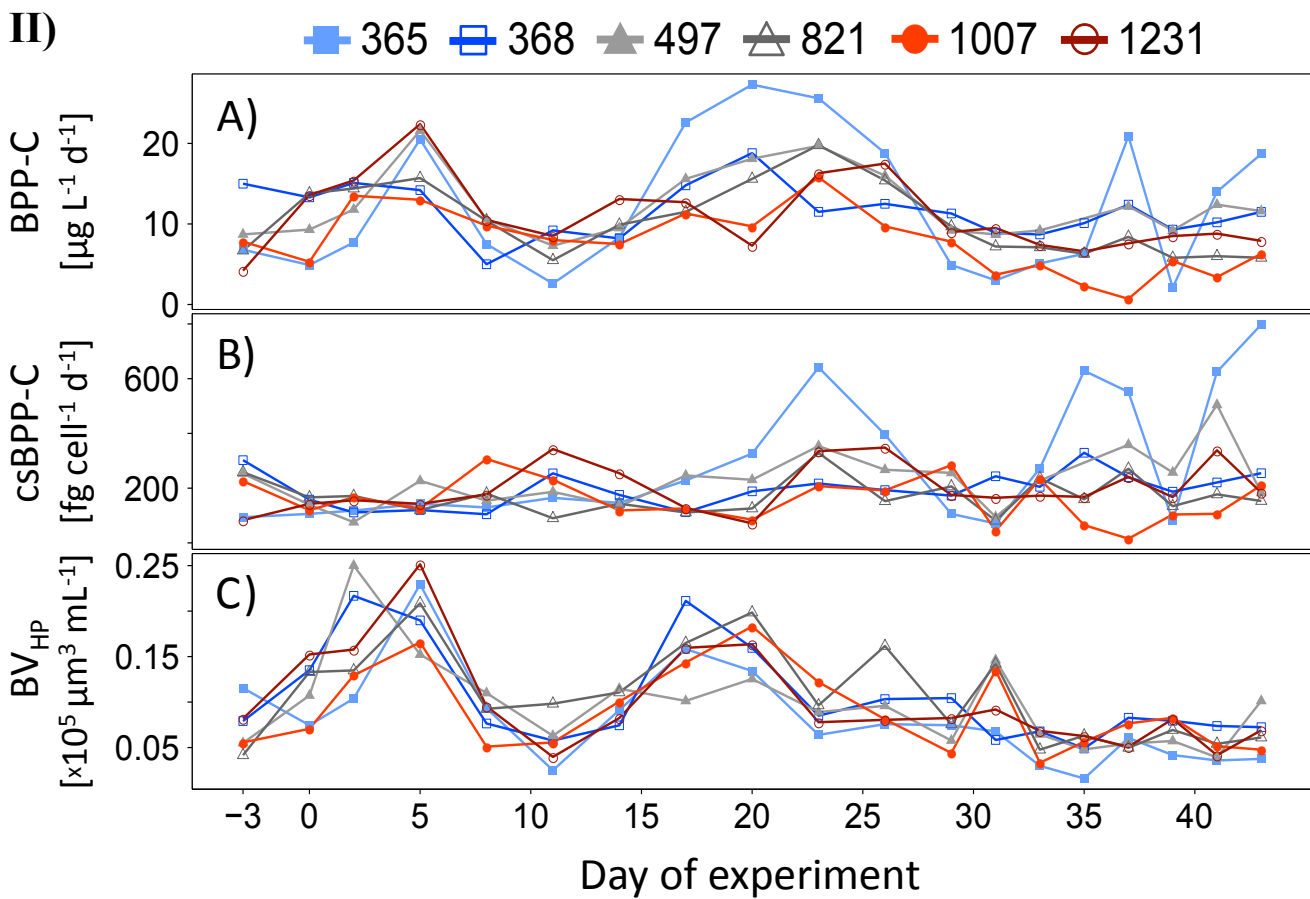
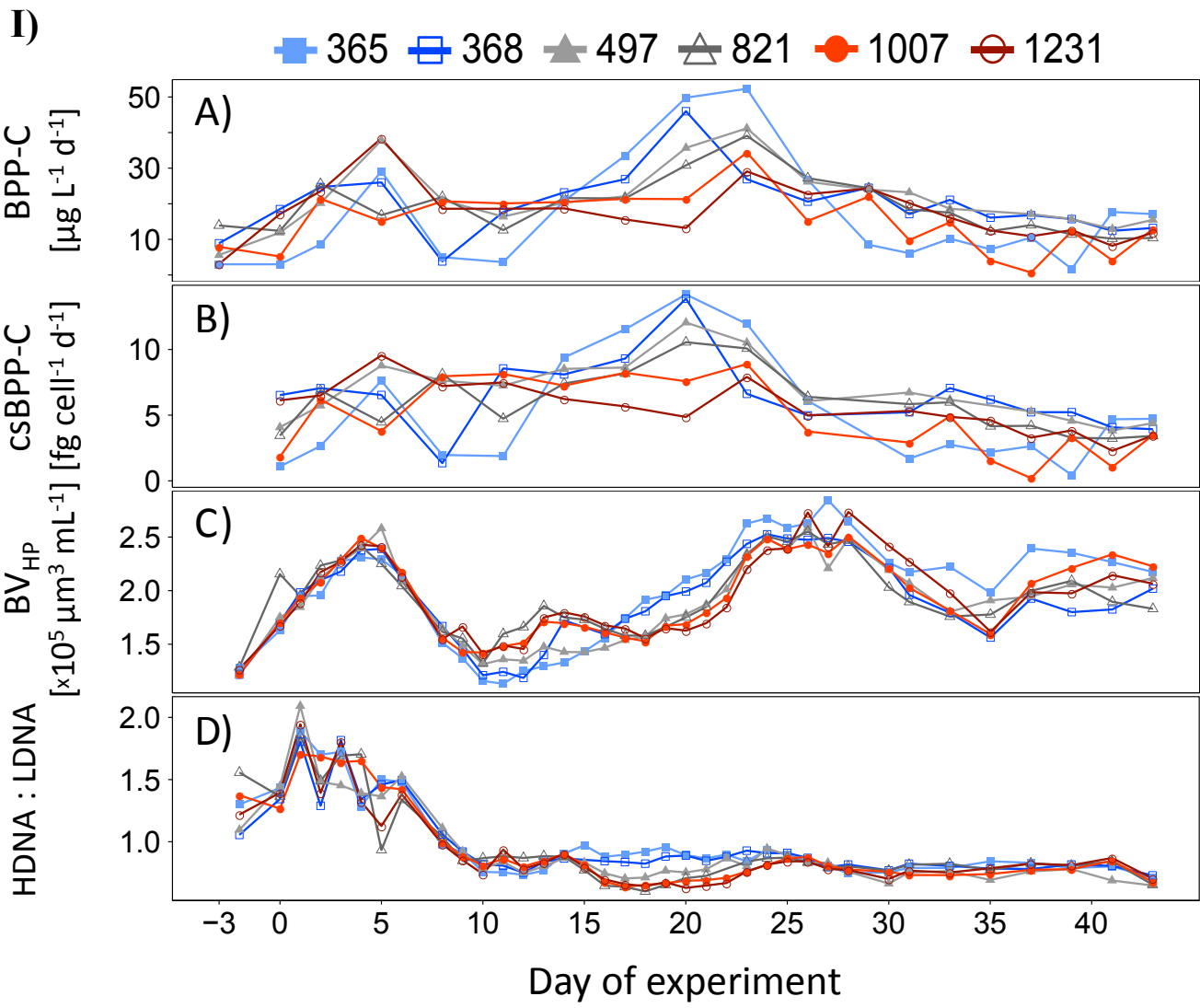


Figure 1. A) Bacterial Protein Production (BPP-C) [$\mu\text{g L}^{-1} \text{d}^{-1}$], B) cell-specific Bacterial Protein Production (csBPP-C) [$\text{fg cell}^{-1} \text{d}^{-1}$] and C) biovolume of heterotrophic prokaryotes (BV_{HP}) [$\times 10^5 \mu\text{m}^3 \text{ml}^{-1}$] of size fractions I) 0.2-5.0 μm (free-living bacteria) and II) $>5.0 \mu\text{m}$ (particle-associated bacteria) during the course of the experiment. I-D) Ratio of high versus low nucleic acid stained prokaryotic heterotrophs (HDNA:LDNA), which both made up free-living BV_{HP} , revealed from flow cytometry. Colours and symbols indicate average $f\text{CO}_2$ [μatm] between t1-t43.

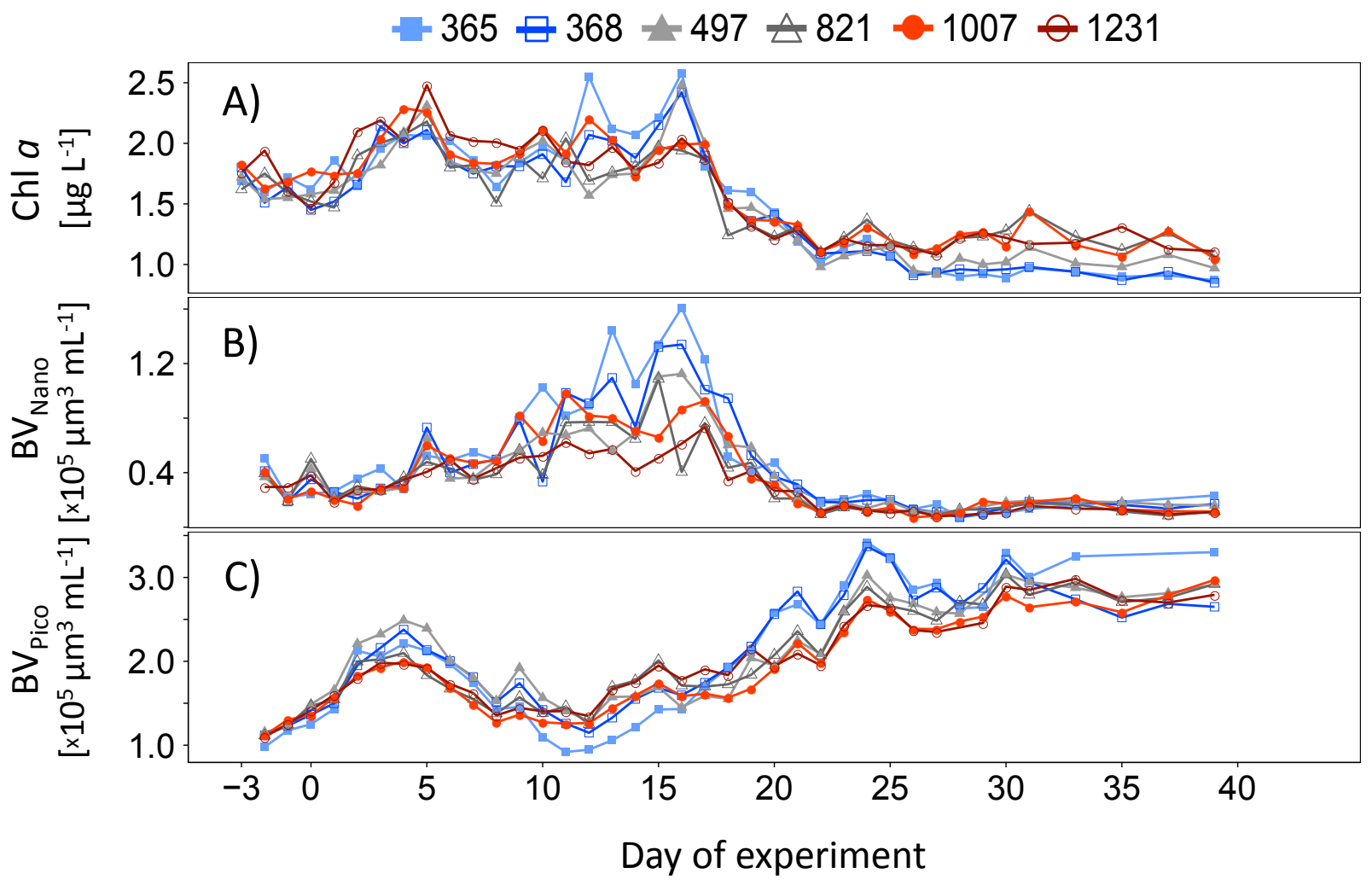


Figure 2. A) Concentration of chlorophyll *a* [$\mu\text{g L}^{-1}$], B) biovolume of nanophytoplankton (Nano I and Nano II) [$\times 10^5 \mu\text{m}^3 \text{ml}^{-1}$] and C) biovolume of picophytoplankton (*Synechococcus* spp., Pico I-III) [$\times 10^5 \mu\text{m}^3 \text{ml}^{-1}$] during the course of the experiment. Colours and symbols indicate average $f\text{CO}_2$ [μatm] between t1-t43.

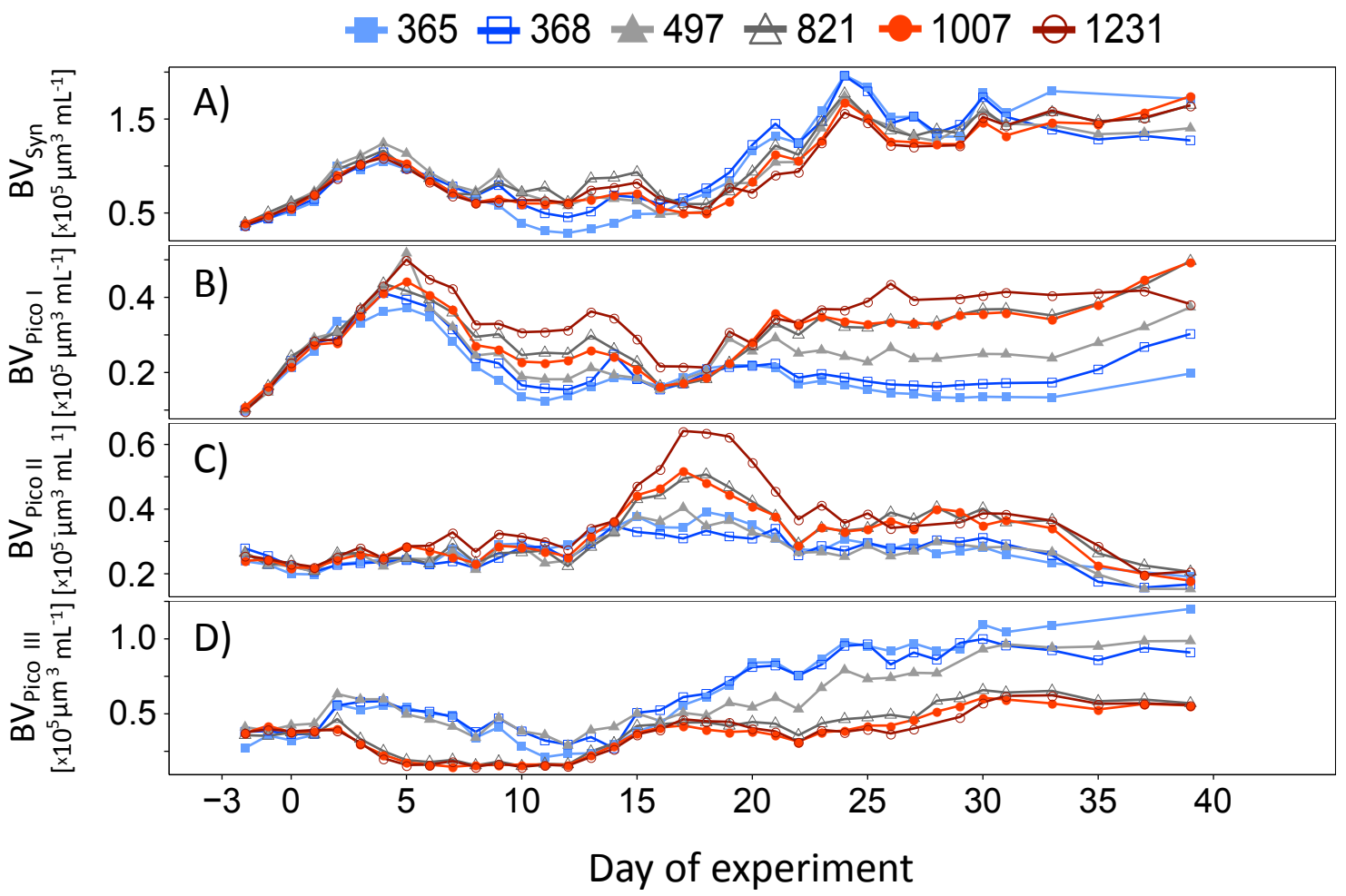


Figure 3. A) Biovolume of *Synechococcus* spp. [$\times 10^5 \mu\text{m}^3 \text{ml}^{-1}$] and B-D) biovolume of picoeukaryote groups I-III (Pico I-III) [$\times 10^5 \mu\text{m}^3 \text{ml}^{-1}$] during the course of the experiment. Colours and symbols indicate average $f\text{CO}_2$ [μatm] between t1-t43.

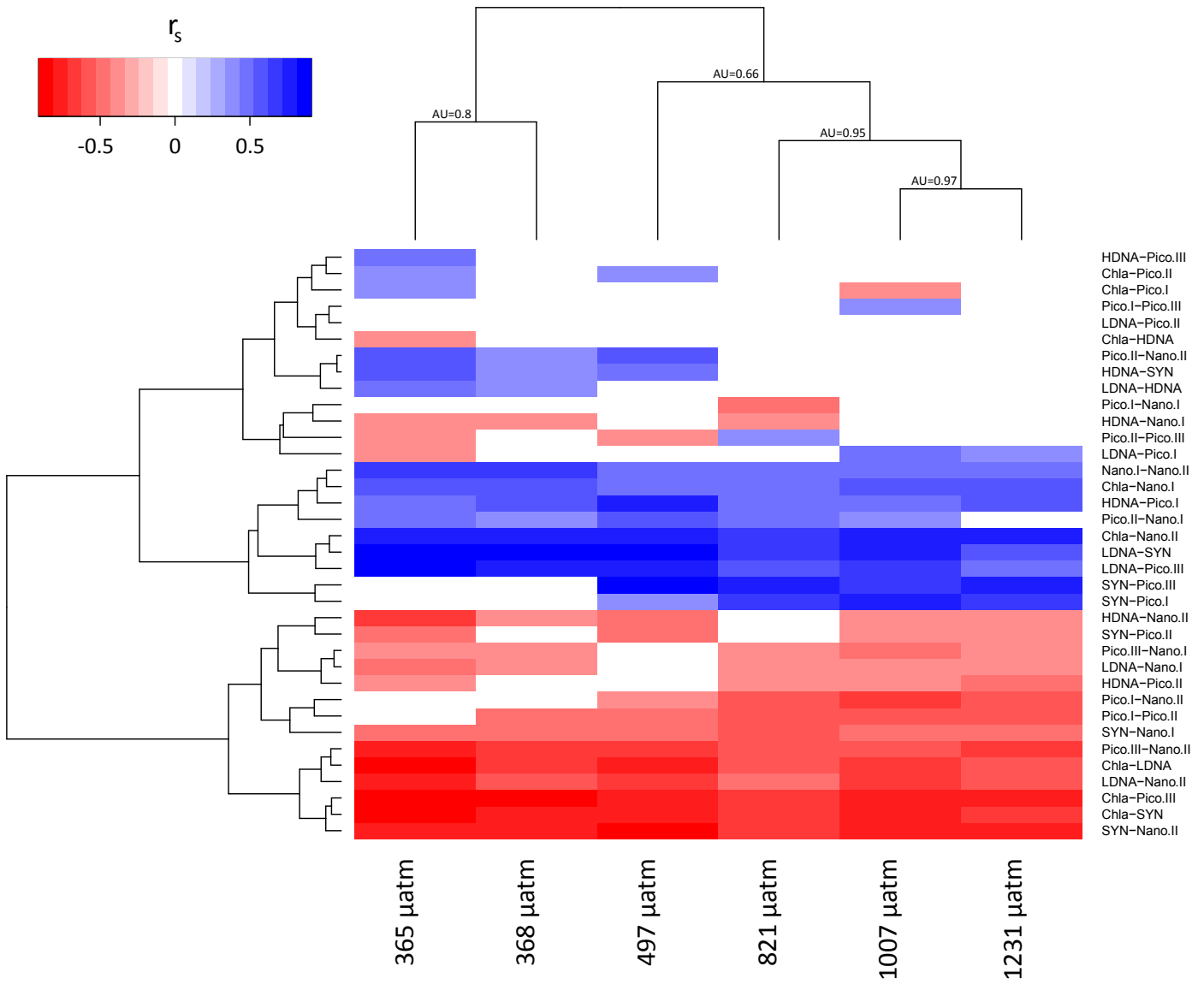


Figure 4. Heatmap and cluster analysis based on significant Spearman`s rank correlation coefficients calculated for each mesocosm between all possible combinations of abundances between different functional heterotrophic prokaryotic and phytoplanktonic groups (high and low nucleic acid stained prokaryotic heterotrophs (HDNA; LDNA), *Synechococcus* spp. (SYN), picoeukaryotes I-III (Pico I-III), nanophytoplankton I-II (Nano I-II)) and Chl *a* based on daily measurements between t1 and t39. Colours indicate the Spearman`s rank coefficient (r_s) between two variables. *P*-values of correlations were corrected for multiple testing according Benjamini and Hochberg (1995). Uncertainty in hierarchical clustering was assessed with multiscale bootstrap resampling using approximately unbiased (AU) *p*-values (between 0 and 1) (Suzuki and Shimodeira, 2015). Clusters of the three highest $f\text{CO}_2$ -treatments are significantly different at the 0.05 level. Numbers indicate the $f\text{CO}_2$ -treatment with average $f\text{CO}_2$ [μatm] between t1-t43.

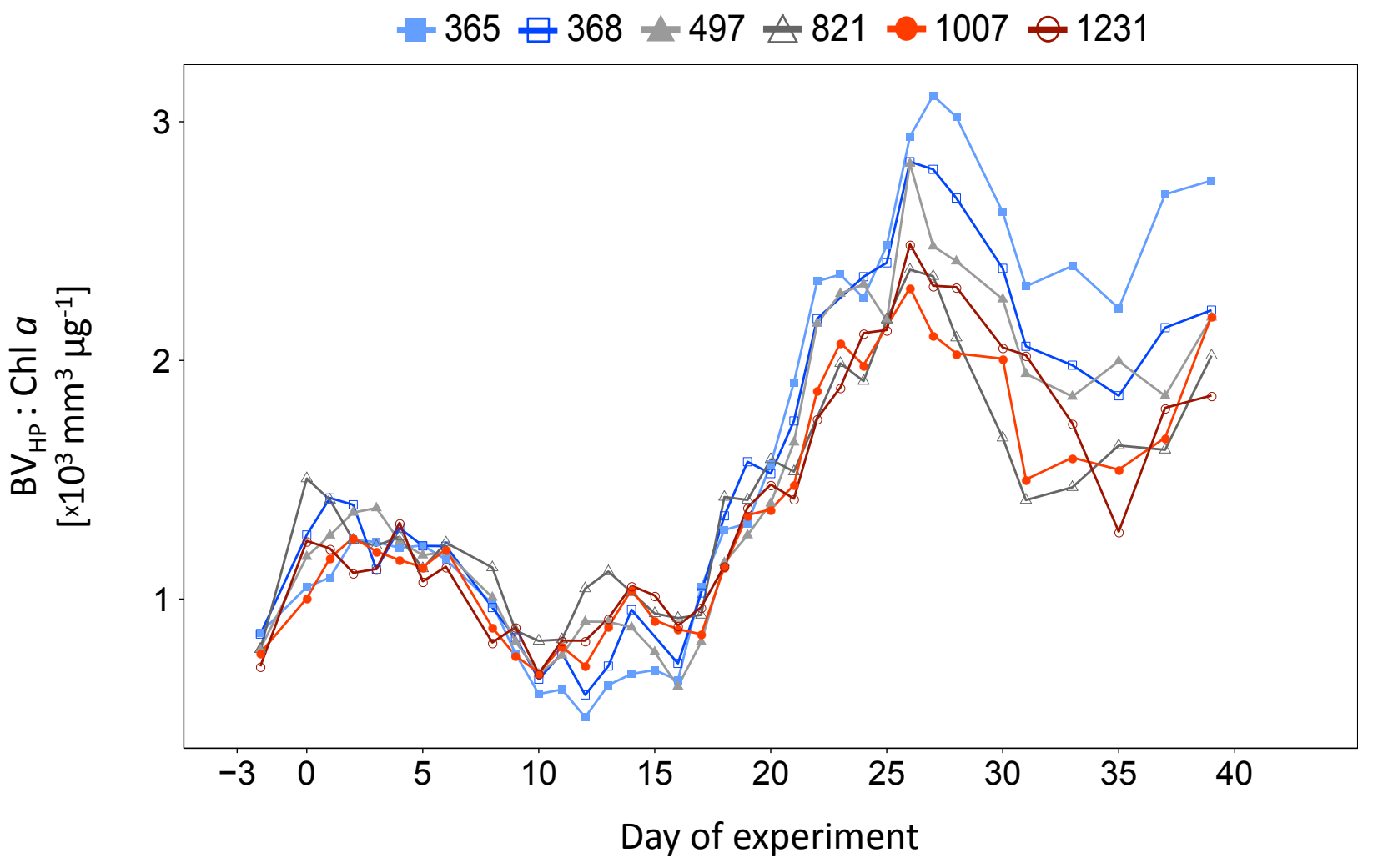


Figure 5. Standardisation of heterotrophic prokaryotic biovolume to total Chl *a* ($BV_{HP} : Chl\ a$) during the course of the experiment. PA BV_{HP} was interpolated using splines with software R (R Core Team, 2016) for time-points, where no data were available. Colours and symbols indicate average fCO_2 [μatm] between t1-t43.

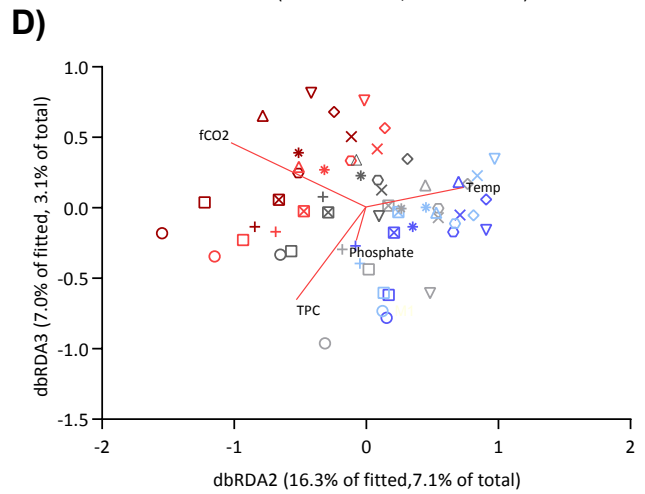
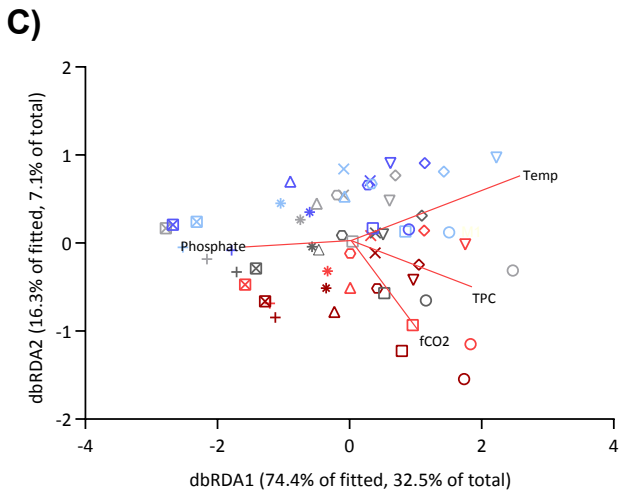
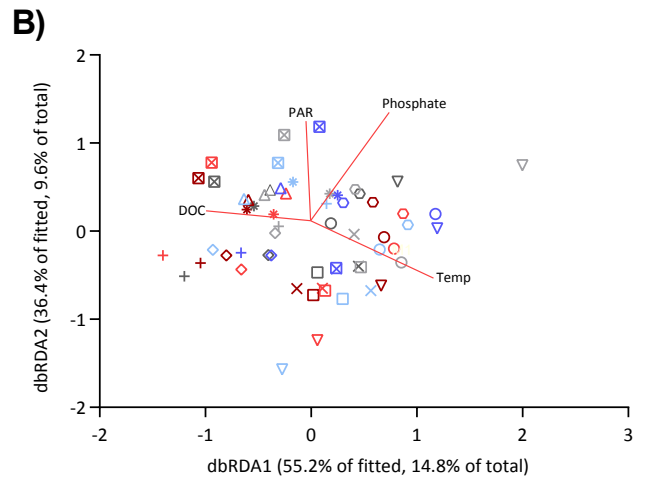
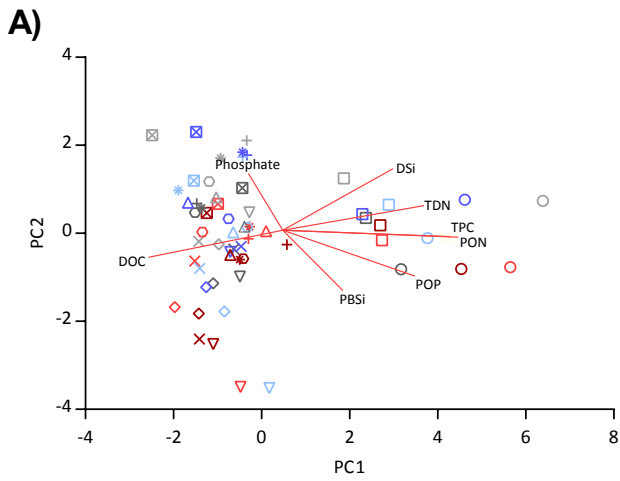


Figure 6. A) First and second axis of a Principal Component Analysis (PCA) calculated on normalized variables of dissolved and particulate nutrients (n=60). The set of variables and the eigenvectors and –values of the first four axes can be derived from Table 2. B) Ordination of a distance-based redundancy analysis (dbRDA) for visual interpretation of distance-based linear modelling (DistLM) between physical/chemical predictor variables and metabolic variable as well as C-D) abundances of functional bacterial and phytoplankton groups. A Table comprising the set of variables used for DistLM can be derived from the Supplementary (Table S1).